A Renal-Like Organic Anion Transport System in the Ciliary Epithelium of the Eye

by

Jonghwa Lee

Submitted in partial fulfilment of the requirements
for the degree of Master of Science

at

Dalhousie University
Halifax, Nova Scotia
December 2014

TABLE OF CONTENTS

LIST OF TABLES…….. v

LIST OF FIGURES…… vi

ABSTRACT……..... vii

LIST OF ABBREVIATIONS AND SYMBOLS USED……... viii

ACKNOWLEDGEMENTS…… xi

CHAPTER 1: INTRODUCTION……..... 1

1.1 Introduction…….. 1

1.2 Drug Transporters……. 2

1.3 Ocular Barriers……..... 4

1.4 In Vivo Evidence for Drug Transporter Function in the Eye…… 5

1.5 Structure of the Ocular Barriers and Drug Transporter Expression and Function…… 6

1.5.1 The Cornea……... 6

1.5.2 The Blood-Aqueous Humor Barrier……. 11

1.5.3 The Blood-Retinal Barrier…… 14

1.6 Drug Metabolism…… 18

1.7 Ocular Drug Metabolism…… 19

1.7.1 Phase I Metabolism in the Eye……. 19

1.7.2 Phase II Metabolism in the Eye…… 21

1.8 Hypothesis…… 22

1.9 Objectives……. 23

CHAPTER 2: MATERIALS AND METHODS…….. 32

2.1 Reagents and Antibodies…….. 32

2.2 Human Tissues……. 33

2.3 Animal Tissues……. 34

2.4 RNA Isolation, RT-PCR and Microarray Analysis…… 34

2.5 SDS-PAGE and Immunoblotting……. 35

2.6 Immunohistochemistry……. 36

2.7 Ussing Chamber Experiments…….. 37

2.8 Statistics…… 39

CHAPTER 3: RESULTS……... 43

3.1 mRNA Expression of Organic Anion Transporters in Ocular Tissues… 43

3.2 Determination of Active Transepithelial PAH Transport Across Ciliary Body……. 44

3.3 Inhibition of Transepithelial PAH Transport Across Ciliary Body…… 45

3.4 Investigation of Active Estrone-3-sulfate and Cidofovir Transport Across Ciliary Body…… 46

3.5 Expression of Organic Anion Transporters in the Ciliary Body…… 46

3.6 Cellular and Subcellular Localization of Organic Anion Transporters in Ciliary Body…… 47

CHAPTER 4: DISCUSSION……. 58

4.1 Overview…….. 58

4.2 Ciliary Body Supports Elimination of Organic Anions from the Eye…. 50

4.3 Transepithelial PAH Transport is Inhibited by Organic Anion Transporter Inhibitors……... 61

4.4 Organic Anion Transporters are Expressed in the Ciliary Body…….. 62

4.5 Predicted Elimination……... 62

4.6 Proposed Mechanism of Ocular Organic Anion Elimination…….. 64

CHAPTER 5: CONCLUSION…….. 69

REFERENCES…… 72

LIST OF TABLES

Table 1.1	Drug transporters in the SLC and ABC families- ligand selectivity and transport mechanism……	25
Table 1.2	Examples of drugs that are OA transporter substrates and that are currently used in treating ocular diseases…….	27
Table 2.1	Oligonucleotide sequence of primers used for RT-PCR……..	40
Table 2.2	Primary antibodies and concentrations used for immunoblotting and immunohistochemistry ……	41

LIST OF FIGURES

Figure 1.1 Three major ocular barrier systems that protect the eye interior from exposure to xenobiotic chemicals outside…… 28

Figure 1.2 Current understanding of drug transporter expression in human corneal epithelium……. 29

Figure 1.3 Current understanding of drug transporter expression in human ciliary body and iris……. 30

Figure 1.4 Current understanding of drug transporter expression in human retina... 31

Figure 2.1 Ussing chamber methodology…….. 42

Figure 3.1 Microarray analysis of OA transporter expression in microdissected human ocular tissues…… 49

Figure 3.2 mRNA expression of organic anion transporters common to kidney in human ocular tissues…… 50

Figure 3.3 Bovine ciliary body supports net active transport of PAH in the aqueous humor-to-blood direction……... 51

Figure 3.4 Transepithelial transport of PAH across the bovine ciliary body in Ussing chambers is inhibited by probenecid…… 52

Figure 3.5 Transepithelial transport of PAH across the bovine ciliary body in Ussing chambers is inhibited by novobiocin…… 53

Figure 3.6 Transepithelial transport of estrone-3-sulfate and cidofovir…… 54

Figure 3.7 mRNA expression of SLC transporters in the ciliary body from four separate human donors……. 55

Figure 3.8 Protein expression of organic anion transporters common to kidney in the ciliary body of four separate human donors…… 56

Figure 3.9 Cellular and subcellular distribution of organic anion transporters in the human ciliary body……. 57

Figure 4.1 The effects of active transport, probenecid inhibition and passive outflow…….. 67

Figure 4.2 Hypothetical model of the involvement of NaDC3, OAT1, OAT3, MRP2 and MRP4 in transepithelial OA transport across the ciliary body, aqueous humor (AH)-to-blood (choroid)……... 68

ABSTRACT

The cornea, blood-retinal barrier and blood-aqueous humor barrier are a significant impediment to ocular drug delivery. These barriers are comprised of endothelial and/or epithelial tissues that act as a physical barrier to drug movement into the intraocular compartment from the outside. There is increasing evidence that these endothelial and epithelial tissues contain drug transporters, and that through active transport they play a functional role in ocular drug disposition as well. Early in vivo and in vitro studies showed that drugs containing a net negative charge at physiological pH (organic anions) are actively eliminated from the eye, with the ciliary body epithelium being a likely site of elimination. An initial screen of drug transporter gene expression by microarray showed that several transporters that contribute to the renal elimination of organic anions are also expressed in the human ciliary body. These included the organic anion transporter 1 (OAT1), organic anion transporter 3 (OAT3), the sodium dicarboxylate cotransporter 3 (NaDC3) and the multidrug resistance-associated protein 4 (MRP4). This led to the hypothesis that the ciliary body epithelium would transport organic anions in the aqueous humor-to-blood direction and that the aforementioned transporters would contribute. The purpose of this study was to determine the direction of organic anion transport across the ciliary body epithelium and the transport proteins that may contribute. Transport of several organic anions across the bovine ciliary body was examined using ciliary body sections mounted in Ussing chambers. RT-PCR, immunoblotting and immunohistochemistry were used to examine organic anion transporter expression in human ocular tissues. mRNA (RT-PCR) and protein (immunoblotting) for OAT1, OAT3, NaDC3 and MRP4 were detected in extracts of human ciliary body from several donors. OAT1 and OAT3 localized to basolateral membranes of non-pigmented epithelial cells and MRP4 to basolateral membranes of pigmented cells in human eye. *Para*-aminohippurate and estrone-3-sulfate transport across the bovine ciliary body in Ussing chambers was greater in the aqueous humor-to-blood direction than in the blood-to-aqueous humor direction, and active. In contrast, there was little net directional movement of cidofovir. Probenecid (0.1 mM) and novobiocin (0.1 mM) added to the aqueous humor side of the tissue abolished net active *para*-aminohippurate transport. These data indicate that the ciliary body expresses several organic anion transporters common to the kidney. These transporters are likely involved in clearing potentially harmful endobiotic and xenobiotic organic anions from the eye.

LIST OF ABBREVIATIONS AND SYMBOLS USED

Ci	Curie
^{3}H	Tritium
kDa	Kilodalton
ABC	ATP-binding cassette
AH	Aqueous humor
ARPE-19	Immortalized human retinal pigmented cell
BAB	Blood-aqueous humor barrier
BCRP	Breast cancer resistant protein
BRB	Blood-retinal barrier
CB	Ciliary body
CDCF	5(6)-carboxy-2,'7'-dichlorofluorescein
CL	Clearance
CX	Connexin
CYP	Cytochrome P450
D407	Immortalized human corneal retinal pigmented epithelial cell
GFR	Glomerular filtration rate
Gly-Sar	Glycylsarcosine
HCEpiC	Primary human corneal epithelial cell
HCE	Human corneal epithelial cell
HEPES	Hydroxyethyl piperazineethanesulfonic acid
HRP	Horseradish peroxidase
IHC	Immunohistochemistry

IOP	Intraocular pressure
I_{sc}	Short-circuit current
kid	Kidney
MATE	Multidrug and toxin extrusion
MRP	Multidrug-resistance associated protein
mw	Molecular weight
NaDC	Sodium-dicarboxylate cotransporter
NKA	Na,K-ATPase
NPT	Sodium-phosphate transporter
OA	Organic anion
OAT	Organic anion transporter
OATP	Organic anion transporting polypeptides
OC	Organic cation
OCT	Organic cation transporter
OCTN	Organic cation transporters novel
PAH	*para*-aminohippurate
PBS	Phosphate buffered saline
PBS-T	PBS-Tween-20
PCR	Polymerase Chain Reaction
PEPT	Peptide transporter
P-gp	P-glycoprotein
PMEA	9-(2-phosphonylmethoxyethyl)adenine
PMT	*N*-methyltransferase
RPE	Retinal pigmented epithelium

RT	Reverse transcriptase
SDS-PAGE	Sodium dodecyl sulfate polyacrylamide gel electrophoresis
SLC	Solute carrier
SV40-HCEC	Immortalized human corneal epithelial cells
TCDD	2,3,7,8-tetrachlorodindibenzo-*p*-digoxin
TLC	Thin-layer chromatography
TPD	Transepithelial potential difference
TER	Transepithelial resistance
URAT	Urate transporter

ACKNOWLEDGMENTS

I would like to gratefully thank my supervisor, Dr. Ryan Pelis, for his guidance and the opportunity to work in his lab. Dr. Pelis has been an excellent supervisor. I am grateful for his patience, kindness and encouragement throughout my degree. He has taught me techniques that I will use for the rest of my career and provided me a bright path for becoming a scientist. I sincerely thank him for the time he has devoted to me and everything that I have learned from his laboratory.

To all the members of the Pelis lab, Leslie Ingraham, Dr. Mansong Li and Dr. Adam Hotchkiss, thank you for being there for me. I truly appreciate your time for helping me both technically and emotionally, and most importantly, for being great friends. I would like to thank Dr. Miguel Coca-Prados at the Department of Ophthalmology and Visual Sciences, Yale University, for the microarray transporter gene expression data to get me started on this project. I also would like to thank Oulton's Farm (Windsor, NS, Canada) for supplying bovine eyes, Dr. Frans G. Russel of Radboud University, Nijmegen Medical Centre for providing the antibody against MRP4, and the staff at the Capital Health Regional Tissue Bank for assistance with acquiring human donor eyes.

I would like to extend my thanks to my advisory committee, Dr. George Robertson and Dr. James Fawcett, for their support and advice throughout my degree. To the staff of the Department of Pharmacology, Luisa Vaughan, Sandi Leaf and Cheryl Bailey, thank you for your help with administrative tasks and for answering my endless questions. Thank you also to Dr. Chris Sinal and the rest of the faculty and technicians in the department for letting me use your labs and equipment over the course of my degree. I would like to thank Stephen Whitefield of the Cellular and Molecular Digital Imaging Facility for providing laser confocal microscope training. I would also like to extend my thanks to my thesis examiners, Dr. Kishore Pasumarthi and Dr. Kerry Goralski, for their time for reviewing my thesis.

Finally, to my family and friends, thank you so much for your support, encouragement and understanding throughout my life. Without them, I could never succeed in my degree.

CAHPTER 1: INTRODUCTION

1.1 Introduction

The eye is a pharmacological sanctuary consisting of three major ocular barriers that physically separate the interior of the eye from the outside – the cornea, the blood-retinal barrier and the blood-aqueous humor barrier (**Fig 1.1**). They protect the ocular tissues from entry of chemicals, making it challenging to treat many ocular diseases with therapeutic drugs. The resilience of the eye to drug exposure is evident from the number of ocular drug delivery methods in development and use, such as intravitreal injection, sustained release implants, nanoparticles, iontophoresis, pro-drugs and magnetic intraocular inserts. Topical, systemic, periocular, and intraocular are the four basic routes for drug delivery to the eye (Geroski and Edelhauser, 2000). Therapeutic concentrations can be achieved with both topical and systemic administration, but often requires the use of relatively high doses and drugs with sufficient hydrophobicity to efficiently cross the blood ocular barriers (Barar et al., 2008;Gaudana et al., 2010). Effective topical delivery is further confounded by pre-corneal factors, including tear film, blinking, tear turnover and induced lacrimation, resulting in aqueous humor bioavailability following topical administration of less than ~5% (Gaudana et al., 2010;Kuno and Fujii, 2011). Periocular and intraocular administration (e.g., ampicillin and ganciclovir administered by intravitreal injection) are used to avoid issues associated with poor drug penetration across the blood ocular barriers. However, once inside, the elimination rate of select drugs is rapid, often necessitating the use of high doses and/or repeated administration to

counteract short drug half-lives (Geroski and Edelhauser, 2000;Yasukawa et al., 2005). The poor intraocular penetration of drugs administered outside of the eye and their rapid elimination once inside suggests that active mechanisms contribute, along with passive processes, to poor ocular drug delivery. Indeed, there is evidence that drug transporters expressed in ocular tissues can function to reduce the intraocular bioavailability of systemically and topically administered drugs, and can facilitate their elimination from both the aqueous and vitreous humor. Presented here is the current understanding of drug transporter expression and function in the ocular barriers and its potential impact on ocular pharmacokinetics. Emphasis is placed on expression of pertinent drug transporters (**Table 1.1**) in native human tissues, as there are apparent differences in expression among species (Zhang et al., 2008), and between native tissue and cell lines (Vellonen et al., 2010;Xiang et al., 2009). Due to limited data on function in native human tissues, functional data comes mostly from human cell lines and from native tissue from other species. Given its importance in pharmacokinetics, also discussed is the current understanding of drug metabolism in ocular tissues, albeit there is limited information on the subject.

1.2 Drug Transporters

Drug transporters predominately support flux across plasma membranes of relatively small (approximately 1000 molecular mass or less) organic molecules that are structurally diverse. Many of these molecules are organic electrolytes that display a net negative charge (organic anions), a net positive charge (organic cations), or both negative and positive charges (zwitterions) at physiological pH. Included within this class of

chemicals are pharmacologically and toxicologically relevant xenobiotics along with endogenous chemicals of physiological importance (Klaassen and Aleksunes, 2010). Due to their charge at physiological pH, efficient movement of organic electrolytes across plasma membranes requires facilitated transport. Drug transporters are expressed in a variety of barrier epithelia/endothelia, such as the intestinal epithelium, liver hepatocytes, kidney tubules and brain capillary endothelium (Klaassen and Aleksunes, 2010). Drug transporters are contained within two distinct families, the solute carrier (SLC) family and the ATP-binding cassette (ABC) family. Transporters in the ABC family use energy in the form of ATP hydrolysis to facilitate efflux of their substrates out of cells (Klaassen and Aleksunes, 2010). The multidrug resistance associated proteins (MRPs), breast cancer resistant protein (BCRP; ABCG2) and P-glycoprotein (P-gp; ABCB1) are drug transporters contained within the ABC family. SLC drug transporters use a variety of energetic mechanisms to support solute flux, including Na^+-dependent co-transport, exchange and electrogenic facilitated diffusion, and can facilitate cellular uptake or exchange depending on the electrochemical gradient of the substrate involved (Pelis and Wright, 2014). Notable examples of SLC drug transporters are the organic anion transporting polypeptides (OATPs), organic anion transporters (OATs), organic cation transporters (OCTs) and multidrug and toxin extrusion transporters (MATEs). A feature of drug transporters is their broad and sometimes overlapping ligand selectivity. SLC and ABC drug transporters likely evolved with increasing physiological complexity to provide protection from exposure to an increasing diversity of xenobiotics (Eraly et al., 2004). Indeed, many of the SLC and ABC drug transporters have arisen by gene duplication and display unique but also redundancy in ligand selectivity (Eraly et al., 2004;Moitra and Dean, 2011). Within the eye drug transporters likely protect tissues that

are important for vision from exposure to potentially toxic xenobiotics and endobiotics, especially the avascular lens epithelium, the cornea and the retina. **Table 1.1** highlights the drug transporters in the SLC and ABC families, along with their general ligand selectivity, transport mechanism and their direction of transport (cellular uptake or efflux) given the predominating driving forces under physiological conditions. Many of these drug transporters interact with drug classes used to treat ocular disease, such as antibiotics, antivirals, anti-inflammatory drugs, anti-glaucoma drugs and anti-cancer drugs. Examples of drugs currently used for treating ocular diseases that are OA transporter substrates are listed in **Table 1.2**. When discussing the human ortholog of the transporters the acronym used for the transporter is in all capital letters. When discussing transporters from other species the first letter of the acronym is in capital letters with the subsequent ones in lower case letters. For example, the acronym for organic anion transporting polypeptide 1A2 in human and any other species but human is OATP1A2 and Oatp1a2, respectively.

1.3 Ocular Barriers

There are three major ocular barrier systems that protect the eye interior from exposure to xenobiotic chemicals outside – the cornea, the blood-retinal barrier and the blood-aqueous humor barrier (**Figure 1.1**). The cornea physically separates the eye interior from the external environment outside of the body. The blood-retinal and blood-aqueous humor barriers separate the eye interior from the systemic circulation. The uveal and retinal capillaries are the two vascular systems derived from the ophthalmic artery that perfuse the eye. The uveal capillaries make up the vascular beds of the ciliary body,

iris and choroid, whereas the retinal capillaries supply the retina (Alm, 1992). The choroidal capillaries and the capillaries extending into the ciliary processes are fenestrated and are not a barrier to diffusion, whereas the retinal and iridial capillaries are continuous with extensive tight junctions between adjacent cells (Alm, 1992). The blood-retinal barrier resides in the posterior segment of the eye and consists of the retinal capillary endothelium (inner blood-retinal barrier) and the retinal pigmented epithelium (outer blood-retinal barrier) (**Figure 1.1**). The blood-aqueous humor barrier resides in the anterior portion of the eye and is comprised of the ciliary body epithelium and the tight capillary endothelium of the iris (**Figure 1.1**). In vivo data suggests that transporters expressed in the ocular barriers reduce the intraocular bioavailability of systemically and topically administered drugs, and their elimination following intraocular administration.

1.4 In Vivo Evidence for Drug Transporter Function in the Eye

In vivo data indicate that the ocular barriers contribute to forming both a physical and functional (transporter-mediated) barrier to drug penetration into the eye from the outside, but also, through both active and passive (aqueous humor outflow) transport, contribute to the intraocular elimination of drugs. The P-gp substrate cyclosporine A administered orally to rabbits at high doses is not detected in intraocular tissues, except when the ocular barriers are disrupted by inflammation (BenEzra and Maftzir, 1990). Hosoya et al., (Hosoya et al., 2009) used microdialysis to examine the movement of the Oat/Oatp substrates benzylpenicllin, mercaptopurine and *para*-aminohippurate (PAH) from vitreous humor-to-choroidal blood across the retinal pigmented epithelium of anesthetized rats. The elimination rates for all compounds was 2-fold higher than that of

mannitol, which is not actively transported and only crosses the epithelium by passive diffusion, and elimination of each was slowed by several Oat/Oatp inhibitors, such as probenecid and bromosulfopthalein (Hosoya et al., 2009). Following a topical dose to rabbits, the maximum aqueous humor concentration and area under the aqueous humor concentration time curve of the antiviral acyclovir was increased by the Mrp inhibitor, MK571. The half-life of carbenecillin (Barza et al., 1982), fluorescein monglucuronide (Kitano and Nagataki, 1986), iodopyracet (Forbes and Becker, 1960) in the rabbit eye, and cefazolin and carbenecillin in the monkey eye (Barza et al., 1983) following intravitreal administration increased considerably following concomitant administration of probenecid. The elimination of iodopyracet from the rabbit eye is a saturable process with a secretory maximum, consistent with the presence of active transport (Becker and Forbes, 1961).

1.5 Structure of the Ocular Barriers and Drug Transporter Expression and Function

1.5.1 The Cornea

The cornea is divided into the epithelium, stroma and endothelium. The corneal epithelium is the outermost layer and provides the first line of defense to xenobiotic penetration into the aqueous humor (Doane et al., 1978;Ahmed and Patton, 1985;Ahmed et al., 1987). The corneal epithelium is composed of three cell types (**Figure 1.1**): 1) basal columnar cells, in which cell division occurs, 2) wing cells, which lie above the basal cells, and 3) stratified squamous epithelial cells, which are the most differentiated cell type (Grass and Robinson, 1988). The stratified squamous cells, at the cell layer

closest to the corneal surface, contain tight junctions, whereas the other cell types in the corneal epithelium do not (Edward and Prausnitz, 2001). The stratified squamous epithelium is a significant barrier to trans-corneal drug penetration, especially for hydrophilic drugs (Zderic et al., 2004;Yang et al., 2009). The stroma is an acellular layer located beneath the corneal epithelium that constitutes approximately 90% of the total volume of the cornea (Kaye, 1969). It is a fibrous tissue that is predominantly comprised of large collagen fibers embedded in a proteoglycan extracellular matrix (Edward and Prausnitz, 2001). Unlike the corneal epithelium, the stroma, given its hydrophilic properties, is an impediment to trans-corneal diffusion of hydrophobic drugs (Ahmed et al., 1987;Malhotra and Majumdar, 2001). The innermost hexagonal-shaped endothelial cells separate the stroma from the aqueous humor. Tight junctions present in the apical membrane of the corneal endothelium do not completely encircle the cells (Noske et al., 1994), and relatively small molecules can traverse the endothelium via the paracellular pathway (Noske et al., 1994;Prausnitz and Noonan, 1998;Malhotra and Majumdar, 2001). The primary physiological role of the corneal endothelium, through inorganic solute and water transport, is to regulate hydration and transparency of the cornea (Fischbarg and Lim, 1974;Hodson and Miller, 1976). Note – the stroma and endothelium are not included in the model shown in **Figure 1.1** since the epithelium is predominately responsible for the barrier function of the cornea and most active drug transport occurs in this layer (see below).

Two lines of evidence support the conclusion that the squamous epithelial layer is the primary barrier to solute diffusion across the cornea (Mannermaa et al., 2006;Barar et al., 2008). First, horseradish peroxidase injected intravenously diffuses across the endothelium and stroma, and between the basal and wing cells, but its progression to the

apical surface of the corneal epithelium is restricted by the tight junctions between squamous cells (Huang et al., 1989). Second, loss of structural integrity of the squamous epithelium, induced by chemical and/or physical disruption, results in increased permeability of drugs across the corneal epithelium (Zderic et al., 2004;Yang et al., 2009).

Dahlin et al., (Dahlin et al., 2013) showed using gene expression analysis that of the 100 most highly expressed genes in the cornea, 29% are drug transporters. Analysis of TransPortal (UCSF-FDA; http://bts.ucsf.edu/fdatransportal/) drug transporter genes of known importance for drug disposition showed that TransPortal gene expression levels in cornea are 6.1-fold higher than in liver and 1.3-fold higher than in kidney (Dahlin et al., 2013). The most heavily expressed TransPortal ABC drug transporter genes in the cornea were: MRP2 > MRP5 > MRP4 > BCRP > MRP1 > MRP3 (Dahlin et al., 2013). Another study examining mRNA expression by qPCR of MRP1-7, P-gp and BCRP in cornea from four separate donors detected mRNA for MRP1, MRP2, MRP3, MRP5, MRP7, P-gp and BCRP (Chen et al., 2013). Protein for MRP1, MRP2, MRP4, MRP5, MRP6, MRP7 and BCRP were detected in cornea by immunoblotting (Pelis et al., 2009;Vellonen et al., 2010;Chen et al., 2013). MRP1-7, BCRP and P-gp localize to the stratified squamous epithelium (Karla et al., 2009;Vellonen et al., 2010;Chen et al., 2013;Dahlin et al., 2013). MRP5 also localizes to the corneal endothelium (Karla et al., 2009). There are discrepancies regarding expression of ABC transporters in human cornea. For example, Dahlin et al., (Dahlin et al., 2013) were unable to detect MRP1, MRP2 or MRP5 expression in the corneal epithelium by immunohistochemistry, and Becker et al., (Becker et al., 2007) did not detect mRNA (RT-PCR) for MRP1, MRP2 or BCRP. In a study examining expression of MRP1-5, P-gp and BCRP using immunoblotting, only MRP1,

MRP5 and BCRP were detected (Vellonen et al., 2010). These discrepancies are most likely caused by factors including post-mortem degradation of the samples, interindividual differences in expression levels, differences in the antibodies and oligonucleotide primer sets used, as well as issues associated with tissue processing, i.e., the cornea is thick, composed of multiple tissue types (expression gets diluted) and difficult to homogenize.

Primary human corneal epithelial cells (HCEpiC) and immortalized human corneal epithelial cells (HCE cells) were shown to express P-gp and several MRPs – albeit, levels were higher in cultured cells versus native tissue (Vellonen et al., 2010). The intracellular retention of calcein (a P-gp and MRP substrate) in HCEpiC and HCE cells was assessed in the presence of cyclosporine A and verapamil (P-gp inhibitors), as well as MK571 (MRP and P-gp inhibitor) (Vellonen et al., 2010). Consistent with the expression of these transporters in the cultured cells, intracellular calcein retention increased in the presence of all inhibitors tested. Further investigation into MRP-specific activity using 5(6)-carboxy-2,'7'-dichlorofluorescein (CDCF) showed that intracellular CDCF retention in both cell lines increased in the presence of probenecid, an MRP inhibitor. The trans-corneal flux of cyclosporine A (P-gp substrate) across a cultured rabbit corneal cell line was ~3-fold higher in the basal-to-apical direction than the apical-to-basal direction, and the intracellular accumulation of rhodamine 123 (P-gp substrate) in the cells was increased by cyclosporine A, suggesting involvement of P-gp in cellular efflux across the apical membrane of the cells (in the eye interior-to-corneal surface direction) (Dey et al., 2003). MK-571 was shown to inhibit the efflux of 9-(2-phosphonylmethoxyethyl)adenine (PMEA; an MRP5 substrate) from immortalized human corneal epithelial cells (SV40-HCEC) that express MRP5 (Karla et al., 2009).

Compared to ABC transporters, fewer studies have examined SLC drug transporter expression and function in the human cornea. Of note is the relative abundant gene expression for OATP1A2, OATP1B3, OCT3 and OCTN2 in an analysis of TransPortal genes (Dahlin et al., 2013). Zhang et al., (Zhang et al., 2008) showed mRNA expression for PEPT1, PEPT2, OATP2B1, OCT1, OCT3 and OCTN1 in human cornea. Whereas one study failed to detect OAT2 mRNA in human cornea (Zhang et al., 2008), another did observe mRNA expression and localized the protein to the corneal epithelium (Dahlin et al., 2013). The study by Dahlin et al., (Dahlin et al., 2013) suggested that OAT2 may be important for the ocular disposition of acyclovir, which is used to treat ocular herpes infections. PEPT1, PEPT2, OCT1 (Kadam et al., 2013) and OCT3 (Dahlin et al., 2013) localize to the corneal epithelium.

Val-acyclovir is a pro-drug of acyclovir and a substrate of PEPT1, whose intestinal expression increases the oral bioavailability of acyclovir (Yang and Smith, 2013). Consistent with the expression of PEPT1 in the corneal epithelium (Zhang et al., 2008), the permeability of Val-acyclovir across the freshly excised rabbit cornea was saturable, pH-dependent and inhibited by other PEPT ligands including dipeptides, β-lactam antibiotics and angiotensin converting enzymes (Anand and Mitra, 2002). Probenecid- and PAH-sensitive uptake of ketoprofen (Fujii et al., 2013), and NaN_3- and 2,4-dinitrophenol-sensitive uptake of tilisolol (Sakanaka et al., 2006) in cultured rabbit corneal epithelial cells suggest the presence of functional Oat and Oct transporters, respectively.

Together, these data indicate that a number of ABC efflux and SLC uptake drug transporters are expressed in the human cornea, consistent with the poor permeability of

select drugs across the tissue. Whereas ABC efflux transporters likely reduce intraocular bioavailability of topically administered drugs by pumping them to the corneal surface, select SLC uptake transporters, such as PEPT1 and OAT2, could be highjacked to improve bioavailability. **Figure 1.2** summarizes the current understanding of drug transporter expression in human corneal epithelium.

1.5.2 The Blood-Aqueous Humor Barrier

The blood-aqueous humor barrier consists of the ciliary body epithelium and the tight capillary endothelium of the iris. The ciliary body is responsible for the production and secretion of aqueous humor into the eye. The ciliary body forms a ring along the inner wall of the globe and extends posteriorly from the root of the iris to the retina (Nobeschi et al., 2006) (**Figure 1.1**). The ciliary body has two structurally distinct segments, the pars plicata and pars plana. The pars plicata is located anteriorly and is characterized by extensive infoldings called ciliary processes, whereas the pars plana lies between the pars plicata and retina, and lacks infoldings (Caprioli J, 1992). The ciliary body is highly vascularized, supplied by the fenestrated choroidal capillaries. The iridial capillaries are continuous and contain tight junctions, but have a higher permeability than retinal capillaries (Alm, 1992). The ciliary body is not an epithelium per se, but a bilayer comprised of two distinct cell types – a pigmented cell layer and a non-pigmented cell layer. The pigmented cell layer faces the choroidal blood supply, whereas the basolateral membrane of the non-pigmented epithelium contacts aqueous humor. Tight junctions are present in the non-pigmented epithelial cells, but not in the pigmented cells (**Figure 1.1**). The functional significance of this was shown in a study that tracked the diffusion of

horseradish peroxidase out of the fenestrated capillaries after intravenous administration (Freddo et al., 1990). The horseradish peroxidase diffused into the intercellular space between the two cell layers, i.e., the space between the apical membrane of the non-pigmented epithelium and the juxtaposing membrane of the pigmented cells, but its progression into the aqueous humor was prevented by tight junctions of the non-pigmented epithelium.

Of the TransPortal ABC drug transporter genes, MRP5, P-gp, BCRP, MRP4 and MRP1 are the most heavily expressed (mRNA level) in human ciliary body, and P-gp, MRP4, MRP5 and MRP1 in iris (Dahlin et al., 2013). Chen et al., (Chen et al., 2013) used qPCR and immunoblotting of native human iris-ciliary body extracts to examine expression of a variety of ABC drug transporters (MRP1-7, P-gp and BCRP). Detected at the mRNA level were MRP1, MRP2, MRP4, MRP5, MRP7, P-gp and BCRP, and protein for MRP1, MRP2, MRP6, MRP7, P-gp and BCRP was observed, with apparent inter-individual differences in expression levels (Chen et al., 2013). Another study also detected mRNA for P-gp, BCRP and MRP1 in iris-ciliary body preparations (Zhang et al., 2008). Since the studies by Zhang et al., (Zhang et al., 2008) and Chen et al., (Chen et al., 2013) used preparations containing both the iris and ciliary body, no conclusion can be made regarding the tissue, cellular and subcellular distribution of the transporters from these studies – note, the study by Dahlin et al., (Dahlin et al., 2013) used ciliary body only. Using microdissection Pelis et al (Pelis et al., 2009) was able to examine protein expression by immunoblotting of P-gp, BCRP, MRP4, MRP2 and MRP1 in the ciliary body and iris. All transporters examined were observed in human ciliary body, and all but P-gp were detected in iris – albeit, expression levels were much weaker in iris. Within the ciliary body MRP2 localizes to the apical membrane of non-pigmented

epithelial cells where it is speculated to function in translocating its substrates from the intracellular compartment into the choroidal blood supply (Pelis et al., 2009).

Information on ABC transporter function in ciliary body is to my knowledge limited to one study that examined Mrp function in primary cultured porcine non-pigmented epithelium (Pelis et al., 2009). Importantly, similar to human MRP2, porcine Mrp2 localized to basolateral membrane of non-pigmented epithelium. Mrp2 was detected in the primary cultured porcine non-pigmented epithelial cells and the efflux of several Mrp2 substrates including CDCF, doxorubicin, calcein and glutathione methylfluorescein was reduced by a variety of Mrp inhibitors, including MK571 (Pelis et al., 2009).

OATP1B3, OATP1A2, OCT2 and OCTN2 are the TransPortal SLC drug transporter genes identified by Dahlin et al., (Dahlin et al., 2013) as most heavily expressed in ciliary body. A study by Zhang et al., (Zhang et al., 2008) showed mRNA expression of PEPT1 (low level), PEPT2, OCT1, OCT2, OCT3, OCTN1, OCTN2, OAT1, OAT3 and OATP2B1 in iris-ciliary body preparations, but interestingly, did not detect OATP1A2 or OATP1B3. Protein for OATP1A2, OATP1C1, OATP2B1, OATP3A1 and OATP4A1 were detected in ciliary body extracts by immunoblotting (Gao et al., 2005). The OATPs show apparent regional differences in expression within the ciliary body. OATP1A2, OATP1C1, OATP2B1, OATP3A1 and OATP4A1 localize to basolateral membrane of non-pigmented epithelial cells in the pars plana, but only OATP2B1, OATP3A1 and OATP4A1 were detected in the pars plicata, where they occur in basolateral membranes of non-pigmented epithelium (Gao et al., 2005). PEPT1, PEPT2 and OCT1 localize to the basolateral membrane of non-pigmented epithelium (Kadam et al., 2013).

Several lines of evidence suggest that OATs, OATPs and OCTs contribute to organic solute uptake into ciliary body, iris or both. In vitro iris-ciliary body segments from the rabbit accumulate the Oat and/or Oatp substrates iodopyracet (Sugiki et al., 1961), prostaglandin F2α (Bito, 1972) and chlorophenol red (Becker, 1960) in a temperature-dependent and saturable manner, and accumulation is inhibited by metabolic poisons and Oat/Oatp inhibitors (Sugiki et al., 1961;Bito, 1972;Becker, 1960). The Oat1 substrate, PAH, actively accumulates in monkey ciliary body preparations, with tissue-to-bath ratios of ~6-7 (Stone, 1979). The substrate of Oat1 and Oat3, 6-carboxyfluorescein, is preferentially transported in the aqueous humor-to-blood direction across rabbit iris-ciliary body in Ussing chambers (Kondo and Araie, 1994). Several fixed quaternary ammonium cations accumulate in iris-ciliary body preparations from the rabbit in a temperature- and metabolic poison-sensitive manner, suggesting involvement of Oct transporters in organic cation uptake (Barany, 1976). **Figure 1.3** summarizes the current understanding of drug transporter expression in human ciliary body and iris.

1.5.3 The Blood-Retinal Barrier

The retina is a highly specialized neural tissue with a unique vascular system that is located in the posterior segment of the eye between the vitreous humor and the choroid. It can be divided into eight layers, with each layer formed by distinct cell types – the layers include the nerve fiber layer, ganglion cell layers, inner plexiform layer, inner nuclear layer, outer plexifrom layer, outer nuclear layer, photoreceptor layer and retinal pigmented epithelium (Erickson et al., 2007). In humans, there are two sources of blood

supply to the retina – the central retinal artery and the choroidal blood vessels (Erickson et al., 2007;Pournaras et al., 2008;Campbell and Humphries, 2012). The branches derived from four branches of the central retinal artery originating at the nerve head supply approximately two thirds of the inner retinal layers. The physiological requirements of the remaining outer retina are supplied by the choroidal vessels, the highly permeable capillary network that perfuse the apical membrane of retinal pigmented epithelial cells.

The blood-retinal barrier consists of the retinal capillary endothelium (inner blood-retinal barrier) and the retinal pigmented epithelium (outer blood-retinal barrier). Both the inner and outer-blood retinal barriers are important for regulating solute and fluid content of the retina (Campbell and Humphries, 2012). The capillaries of the inner blood-retinal barrier have an ultrastructure similar to brain capillaries in that they both contain extensive tight junctions (Alm, 1992). Due to the presence of tight junctions, unlike the leaky vasculature of choroidal blood vessels, the inner blood-retinal capillary endothelium has low passive paracellular permeability, even to small molecules, such as sodium ions (Tornquist et al., 1990;Chen et al., 2008). The outer blood-retinal barrier consists of the retinal pigmented epithelium that contains extensive tight junctions, with its apical membrane facing the choroidal blood supply and basolateral membrane facing the retina (Cohen AI, 1992). The retinal pigmented epithelium controls the movement of solutes and nutrients from the choroid to the retina.

Dahlin et al., (Dahlin et al., 2013) reported that TransPortal gene expression levels in retina are 4.08-fold higher than in liver and 0.69-fold the level of that observed in kidney. The most highly expressed TransPortal ABC drug transporter genes are P-gp, MRP5, BCRP and MRP1 (Dahlin et al., 2013). mRNA for MRP1, MRP2, MRP3, MRP4,

MRP5, MRP7, P-gp and BCRP were detected in human retina-choroid extracts by qPCR (Zhang et al., 2008;Chen et al., 2013), and protein for MRP1, MRP2, MRP5, MRP6, MRP7, P-gp and BCRP were detected by immunoblotting (Chen et al., 2013).

Using microdissected retinal pigmented epithelium, presumably to be largely devoid of retina and choroid, protein expression for P-gp, BCRP, MRP4, MRP2 and MRP1 were detected in retinal pigmented epithelium (Pelis et al., 2009). P-gp localizes to both apical and basolateral membranes of retinal pigmented epithelium (Kennedy and Mangini, 2002). These data suggest that the efflux of P-gp substrates occurs in the direction of both choroid and retina.

P-gp expression was also detected in primary cultured human retinal pigmented epithelial cells and immortalized human retinal pigmented epithelial cells (D407), and the uptake of rhodamine 123 (a P-gp substrate) in these cells was increased in the presence of P-gp inhibitors (Kennedy and Mangini, 2002;Constable et al., 2006). D407 cells, and another immortalized human retinal pigmented cell line, ARPE-19, express MRP1, MRP4 and MRP5 (Mannermaa et al., 2009). Unlike the D407 cells, the ARPE-19 cells do not express P-gp, and functional activity of MRP efflux transporters in the ARPE-19 cells was demonstrated using calcein (P-gp and MRP substrate) and CDCF (MRP substrate) (Mannermaa et al., 2009). In this study the intracellular retention of calcein and CDCF was increased by the MRP inhibitor probenecid. Compared to the inward permeability (choroid-to-retina), the outward permeability (retina-to-choroid) of verapamil and rhodamine (P-gp substrates) across the porcine retinal pigmented epithelium was ~3-fold higher (Steuer et al., 2005). The permeability of calcein and fluorescein across the porcine retinal pigmented epithelium was also greater in the retina-

to-choroid direction, and reduced by verapamil and probenecid, suggesting P-gp and Mrp involvement, respectively (Steuer et al., 2005).

The most highly expressed TransPortal SLC drug transporters in retina are OATP1B3, OATP1A2, OCT2, OCT3 and OCTN2 (Dahlin et al., 2013). Zhang et al. (Zhang et al., 2008) used qPCR of human native retina-choroid extracts to examine expression of a variety of SLC drug transporters. They detected PEPT2, OCT1, OCT3, OCTN1, OCTN2, OAT2, OAT3 and OATP1A2, but not OCT2 or OATP1B3. Information on SLC transporter localization in the human retina is limited. PEPT1, PEPT2, OCT1 (Kadam et al., 2013) and OCT3 (Dahlin et al., 2013) were localized to retinal pigmented epithelium, but their subcellular localization was not determined.

Approximately 4-fold higher outward (vitreous humor-to-blood) permeability compared to the inward (blood-to-vitreous humor) permeability of fluorescein and its glucuronide was reported using in vitro retinal pigmented epithelium-choroid preparations from the rabbit (Koyano et al., 1993). The outward permeability was inhibited by metabolic poisons and Oat/Oatp inhibitors, and the net movement was saturable and temperature-sensitive. Tsuboi et al., (Tsuboi and Pederson, 1986) also demonstrated fluorescein and carboxyfluorescein transport across isolated dog retinal pigmented epithelium-choroid. Outward permeability was 47- and 9-fold higher than inward permeability for fluorescein and carboxyfluorescein, respectively, and no statistical difference between outward and inward permeabilities for both substrates was observed in the presence of probenecid. Transport of Gly-Sar (PEPT substrate) and 1-methyl-4-phenylpyridinium (OCT substrate) across sclera-choroid-retinal pigmented epithelium preparations occurred preferentially in the sclera-to-retina direction and was inhibited by PEPT and OCT inhibitors, suggesting that PEPT's and OCT's may facilitate

retinal drug delivery (Kadam et al., 2013). **Figure 1.4** summarizes the current understanding of drug transporter expression in human retina.

1.6 Drug Metabolism

Drug metabolism is the process by which the body enzymatically modifies a compound making it more readily eliminated from the body by urinary or biliary excretion. Most drug metabolism occurs in liver hepatocytes, although there are many other tissues with the capacity for drug metabolism, such as epithelia in the gut and lungs, and even in the blood (Litterst et al., 1975;Krishna and Klotz, 1994). The process of drug metabolism is generally divided into two phases, Phase I and Phase II, but the reactions do not necessarily occur sequentially. Phase I reactions include *N*- and *S*-oxidation, *N*- and *S*-dealkylation, aliphatic and aromatic hydroxylation and deamination (Jancova et al., 2010;Li and Bluth, 2011;Pereira, I and Bernkop-Schnurch, 2014). They transform compounds into more polar metabolites by adding or unmasking functional groups, such as –OH, $–NH_2$, –SH and $–CO_2H$, and these functional groups serve as potential sites of Phase II reactions. Phase II metabolic reactions are the conjugation reactions. The parent drug and/or the metabolite formed as a consequence of phase I reactions may be subject to conjugation reactions. These reactions produce, by glucuronidation, sulfation, glutathione-conjugation, *N*-acetylation and methylation, metabolites that are more readily excreted from the body (Jancova et al., 2010;Pereira, I and Bernkop-Schnurch, 2014).

1.7 Ocular Drug Metabolism

Early studies using animal tissue homogenates prepared from the cornea, retina and ciliary body suggest that Phase I and II enzymes are present in ocular tissues (Ross et al., 1975;Shichi and Nebert, 1982). Data on metabolism of endogenous and exogenous substrates in ocular tissues suggest a role for metabolism in ocular drug delivery – preventing entry of and/or eliminating potential toxins from the eye interior (Coupland et al., 1994;Dias et al., 2002;Al-Ghananeem and Crooks, 2007). In addition, there is interest in identifying the enzymes present in the various ocular tissues with the hope of improving ocular drug bioavailability through enzymatic conversion of prodrugs to their active form (Dias et al., 2002;Malik et al., 2012;Vooturi et al., 2012).

1.7.1 Phase I Metabolism in the Eye

Cytochromes P450 (CYPs) constitute a superfamily of heme enzymes that use heme as a cofactor. CYPs are a major source of variability in pharmacokinetics and drug response, and found in all living species (Anzenbacher and Anzenbacherova, 2001;Lynch and Price, 2007;Zanger and Schwab, 2013). The CYP1, 2 and 3 families are responsible for the metabolism of about 70 – 80% of pharmaceutical agents (Gardiner and Begg, 2006;Zanger and Schwab, 2013).

Relatively little is known about CYP expression and activity in ocular tissues, and there is limited data demonstrating CYP involvement in ocular drug metabolism. However, the CYP-dependent metabolism of endogenous substrates, such as arachidonic acid in the ciliary body and retinal pigmented epithelium (Schwartzman et al., 1987), and

prostaglandins in the ciliary body (Asakura and Shichi, 1992), along with the conversion of the amide prodrug of celecoxib to celecoxib in the retina (Malik et al., 2012), suggests that CYPs occur in the blood-ocular barriers and have the potential to contribute to ocular drug delivery. Zhang et al., (Zhang et al., 2008) examined mRNA levels of ten major drug metabolizing CYP enzymes in various tissues in human eye with respect to their levels in the liver. Notably, CYP2A6 and 2D6 were detected in the cornea, iris-ciliary body and retina-choroid, but levels were much lower than in the liver. Another study examining mRNA expression by RT-PCR of a variety of CYPs and genes associated with regulation of CYP expression in primary cultures of nonpigmented human ciliary body epithelium detected CYP1A1, 1B1, 2D6, aryl hydrocarbon receptor, aryl hydrocarbon receptor nuclear translocator and the glucocorticoid receptor (Volotinen et al., 2009). Induction of mRNA and protein expression of CYP1B1 by 2,3,7,8-tetrachlorodindibenzo-*p*-digoxin (TCDD) was confirmed by Northern blotting and immunoblotting (Volotinen et al., 2009). CYP1B1 localizes to nonpigmented ciliary body epithelium and the iris in both humans (Doshi et al., 2006) and mice (Zhao and Shichi, 1995).

The significance of drug metabolizing enzymes should not be limited to their role in drug metabolism. CYP1B1 plays a role in eye development and in pathology associated with congenital glaucoma and anterior segment dysgenesis (Doshi et al., 2006;Vasiliou and Gonzalez, 2008;Su et al., 2012). Mutations in the coding region of CYP1B1 cause reduction in protein stability or enzymatic activity, which ultimately results in reduced CYP1B1 activity (Chavarria-Soley et al., 2008;Choudhary et al., 2008). It is not yet clear how CYP1B1 mutations lead to pathology associated with congenital glaucoma and anterior segment dysgenesis (Doshi et al., 2006;Vasiliou and Gonzalez, 2008).

Acetyltransferase and acetylcholinetransferase activities have been reported in the isolated retina of mouse using radiolabeled substrates (Ross et al., 1975). Histochemistry approaches detected monoamine oxidase and hydrolases in various tissues. Monoamine oxidase was detected in the corneal epithelium, iris-ciliary body, and retinal pigmented epithelium (Shanthaveerappa and Bourne, 1964), and its functional activity was confirmed in homogenates of bovine retina (Sparks et al., 1981). Phase I hydrolases, such as β-glucuronidase and β-galactosidase, localize to the corneal epithelium and the ciliary body epithelium in human, porcine and rat eye (Coupland et al., 1994).

1.7.2 Phase II Metabolism in the Eye

Compared to Phase I metabolism, information on expression and functional activity of Phase II metabolizing enzymes in the human eye is limited. Saneto et al., (Saneto et al., 1982) purified two isozymes of glutathione *S*-transferase from bovine retina and demonstrated functional activity of the enzyme by measuring the conjugation of glutathione with 1-chloro-2,4-dinitrobenzene. Histochemical investigation using dissected rabbit and bovine cornea show the presence of alkaline phosphatase in both corneal epithelium and endothelium (Lojda et al., 1976). Functional activity consistent with alkaline phosphatase activity in cornea come from studies using a phosphate ester pro-drug of cannabinoids, which are converted into the active (parent) form following topical administration (Juntunen et al., 2005). There is also evidence of phospholipid *N*-methyltransferase (PMT) activity in the retina. Sastry et al., (Sastry et al., 1994) observed biotransformation of phosphatidylethnolamine into phosphatidylcholine in the presence of the PMT co-factor *S*-adenosyl-L-methionine.

1.8 Hypothesis

Organic anions (OAs) represent a broad class of chemicals that carry a net negative charge at physiological pH, and include molecules of physiological, toxicological and pharmacological significance. Systemically, many OAs are eliminated from the plasma via active transport mechanisms in the kidney tubule and hepatocytes. In vivo studies using intravitreal injection of OAs that are actively eliminated from the body, in part by renal tubular secretion, suggest that, in addition to passive elimination via the outflow pathway (Forbes and Becker, 1961), OAs are also eliminated from the eye by active transport. For example, the half-life of carbenecillin (Barza et al., 1982) and iodopyracet (Forbes and Becker, 1960) in the rabbit eye, and cefazolin and carbenecillin in the monkey eye (Barza et al., 1983), increased considerably following concomitant administration of probenecid, a well-established inhibitor of renal OA transport. Consistent with the presence of an active OA transport system in the eye, the elimination of iodopyracet from the rabbit eye in vivo was a saturable process with a secretory maximum (Becker and Forbes, 1961). What is not apparent from these early in vivo studies are the ocular tissue(s) that contribute to active OA elimination.

There is considerable in vitro evidence that active transport mechanisms for OAs occur in the anterior uvea (ciliary body and iris). Iris-ciliary body preparations from the rabbit accumulate the OAs iodopyracet (Sugiki et al., 1961), prostaglandin F2α (Bito, 1972) and chlorophenol red (Becker, 1960) in a temperature-dependent and saturable manner, and accumulation is inhibited by metabolic poisons and other OAs (Sugiki et al., 1961;Bito, 1972;Becker, 1960). The well-established substrate of the renal OA secretory

system, PAH, actively accumulates in preparations of monkey ciliary body, with tissue-to-bath ratios of ~6-7 (Stone, 1979). Another substrate of the renal OA secretory system, 6-carboxyfluorescein, is preferentially transported in the aqueous humor-to-blood direction across rabbit iris-ciliary body preparations in Ussing chambers (Kondo and Araie, 1994). An initial analysis by microarray of drug transporter genes in microdissected human ocular tissues also indicate that members of the renal OA secretory system are present in the ciliary body (see Chapter 3). Together, these data led to the hypothesis that OA transporters present in the kidney are expressed in the ciliary body and that they contribute to the active elimination of OAs from the aqueous humor.

1.9 Objectives

The purpose of this study was to determine 1) the direction in which the ciliary body transports OAs, 2) if the ciliary body expresses OA transporters common to other barrier epithelia, including the kidney, and 3) if so, their cellular and subcellular distribution. The OA transporters that were examined in detail included organic anion transporter 1 (OAT1; SLC22A6), organic anion transporter 3 (OAT3; SLC22A8), the Na-dicarboxylate cotransporter 3 (NaDC3; SLC13A3) and the multidrug-resistance associated protein 4 (MRP4), as they are major components of the renal OA transport system.

In this study, bovine ciliary body was used as a model system because tissues were readily available and were of an appropriate size to mount in Ussing chambers (ciliary bodies from smaller species were too small for the Ussing chamber apparatus). We cannot rule out the possibility of species differences (human vs. bovine) in ligand

selectivity of the individual OA transporters examined, or in their cellular and subcellular expression in the ciliary body. However, it is important to note that bovine OAT1 and OAT3 were expected to transport PAH and estrone-3-sulfate, respectively, since OAT1 and OAT3 from a variety of species other than human transport PAH and estrone-3-sulfate.

Table 1.1. Drug transporters in the SLC and ABC families- ligand selectivity and transport mechanism

Generic name	Gene name	Ligand selectivity	Transport mechanism	Direction of transport
Organic anion transporters				
OAT1	SLC22A6	Small OAs	Exchange	Uptake
OAT2	SLC22A7	Small OAs	Exchange	Uptake
OAT3	SLC22A8	Small OAs	Exchange	Uptake
OAT4	SLC22A11	Small OAs	Exchange	Uptake
OAT5	SLC22A10	Small OAs	Exchange	Uptake
OAT7	SLC22A9	Small OAs	Exchange	Uptake
OAT10	SLC22A13	Small OAs	Exchange	Uptake
Urate transporter				
URAT1	SLC22A12	Urate/uricosurics	Exchange	Uptake
Na-phosphate transporters				
NPT1	SLC17A1	OAs/phosphates	Electrogenic uniport	Efflux
NPT4	SLC17A3	OAs/phosphates	Electrogenic uniport	Efflux
Organic anion transporting polypeptides				
OATP6A1	SLCO6A1	Large OAs	Exchange	Uptake
OATP5A1	SLCO5A1	Large OAs	Exchange	Uptake
OATP4A1	SLCO4A1	Large OAs	Exchange	Uptake
OATP3A1	SLCO3A1	Large OAs	Exchange	Uptake
OATP2A1	SLCO2A1	Large OAs	Exchange	Uptake
OATP1C1	SLCO1C1	Large OAs	Exchange	Uptake
OATP4C1	SLCO4C1	Large OAs	Exchange	Uptake
OATP1A2	SLCO1A2	Large OAs	Exchange	Uptake
OATP1B3	SLCO1B3	Large OAs	Exchange	Uptake
OATP1B1	SLCO1B1	Large OAs	Exchange	Uptake
OATP2B1	SLCO2B1	Large OAs	Exchange	Uptake
Organic cation transporters				
OCT1	SLC22A1	OCs	Electrogenic uniport	Uptake
OCT2	SLC22A2	OCs	Electrogenic uniport	Uptake
OCT3	SLC22A3	OCs	Electrogenic uniport	Uptake
Organic cation transporters novel				
OCTN1	SLC22A4	Ergothionine/OCs	Exchange	Uptake

Table 1.1. Drug transporters in the SLC and ABC families- ligand selectivity and transport mechanism

OCTN2	SLC22A5	Carnitine/OCs	Exchange	Uptake
Multidrug and toxin extrusion transporters				
MATE1	SLC47A1	OCs	OC/H Exchange	Efflux
MATE2	SLC47A2	OCs	OC/H Exchange	Efflux
Multidrug resistance-associated proteins				
MRP1	ABCC1	OAs	ATP-hydrolysis	Efflux
MRP2	ABCC2	OAs	ATP-hydrolysis	Efflux
MRP3	ABCC3	OAs	ATP-hydrolysis	Efflux
MRP4	ABCC4	OAs	ATP-hydrolysis	Efflux
MRP5	ABCC5	OAs	ATP-hydrolysis	Efflux
MRP6	ABCC6	OAs	ATP-hydrolysis	Efflux
MRP7	ABCC7	Cl^-/SCN^-	ATP-hydrolysis	Ion Channel
MRP8	ABCC8	Sulfonylurea/K^+	ATP-hydrolysis	Receptor/Ion Channel
MRP9	ABCC8	Sulfonylurea/K^+	ATP-hydrolysis	Receptor/Ion Channel
Breast cancer resistant protein				
BCRP	ABCG2	OAs/OCs	ATP-hydrolysis	Efflux
P-glycoprotein				
P-gp	ABCB1	OCs/OAs/Neutral	ATP-hydrolysis	Efflux

Small OAs < ~500 mw
Large OAs ~500-1000 mw

Table 1.2. Examples of drugs that are OA transporter substrates and that are currently used in treating ocular diseases

Drug classes	Therapeutic drugs	Transporter
Antibiotic	Carbenicillin, Penicillin	P-gp, BCRP, MRP1, MRP2, MRP4, OAT1, OAT2, OAT3, OAT4
Chemotherapeutics	Methotrexate 5-fluorouracil	P-gp, MRP2, MRP4, MRP5, OAT1, OAT3, OAT4
Antivirals	Cidofovir, Ganciclovir	P-gp, BCRP, MRP4, OAT1, OAT3, OCT1, PEPT1
Prostaglandin analogs	Bimatoprost, Latanoprost	P-gp, MRP2, MRP4, MRP5, OAT1, OAT3, OATP2B1

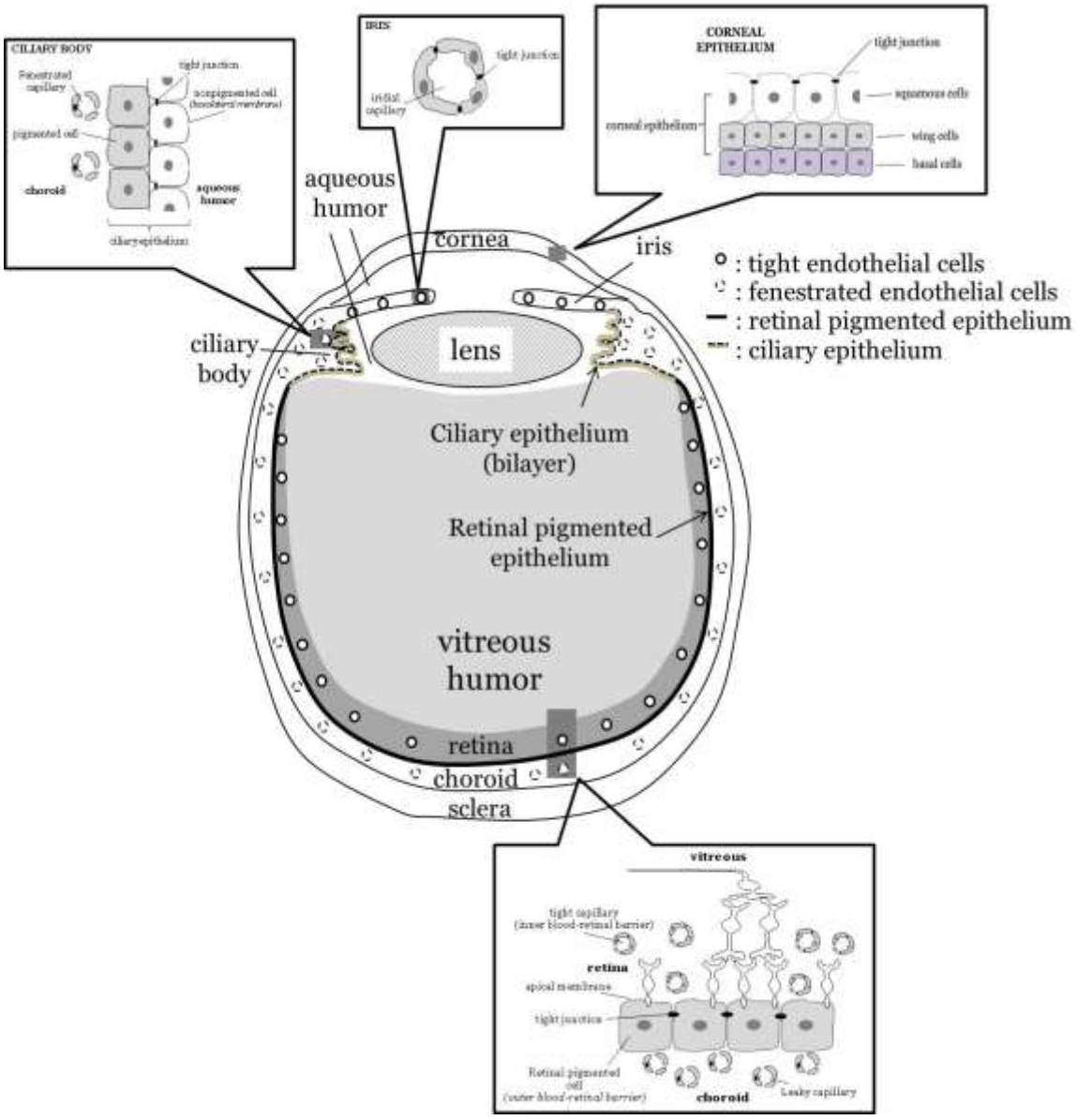

Figure 1.1. Three major ocular barrier systems that protect the eye interior from exposure to xenobiotic chemicals outside – the corneal epithelium, the blood-retinal barrier and the blood-aqueous humor barrier. The corneal epithelium physically separates the eye interior from the external environment outside of the body. The blood-retinal and blood-aqueous humor barriers separate the eye interior from the systemic circulation. The corneal epithelium and the blood-aqueous barrier reside in the anterior segment of the eye. The blood-retinal barrier resides in the posterior segment of the eye.

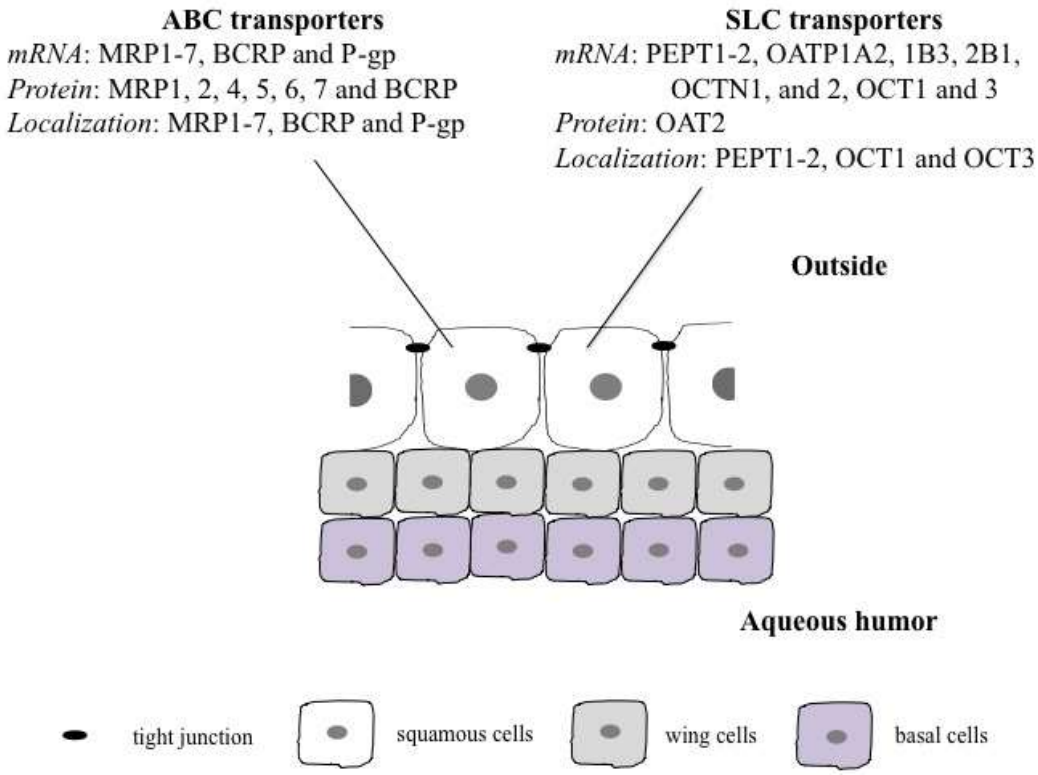

Figure 1.2. Current understanding of drug transporter expression in human corneal epithelium. mRNAs were detected by RT-PCR and/or qPCR. Proteins were detected by immunoblotting. Localization was done using immunohistochemistry. References are given in the text.

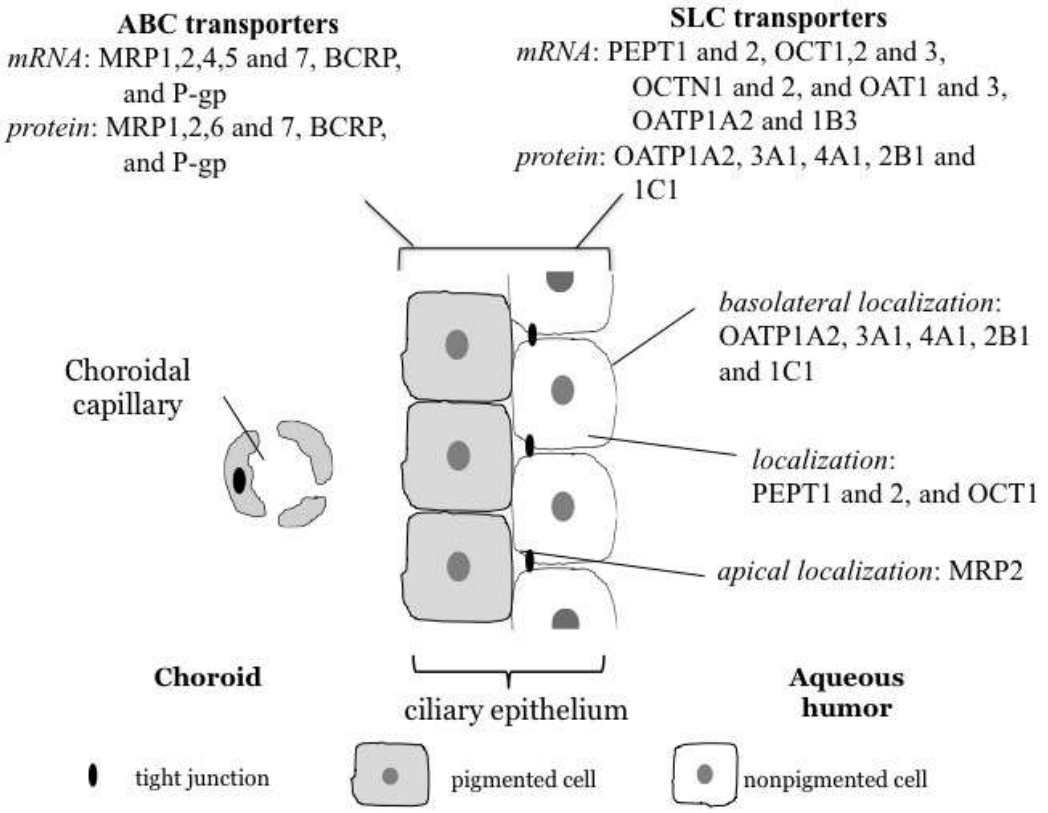

Figure 1.3. Current understanding of drug transporter expression in human ciliary body and iris. mRNAs were detected by RT-PCR and/or qPCR. Proteins were detected by immunoblotting. Localization was done using immunohistochemistry. References are given in the text.

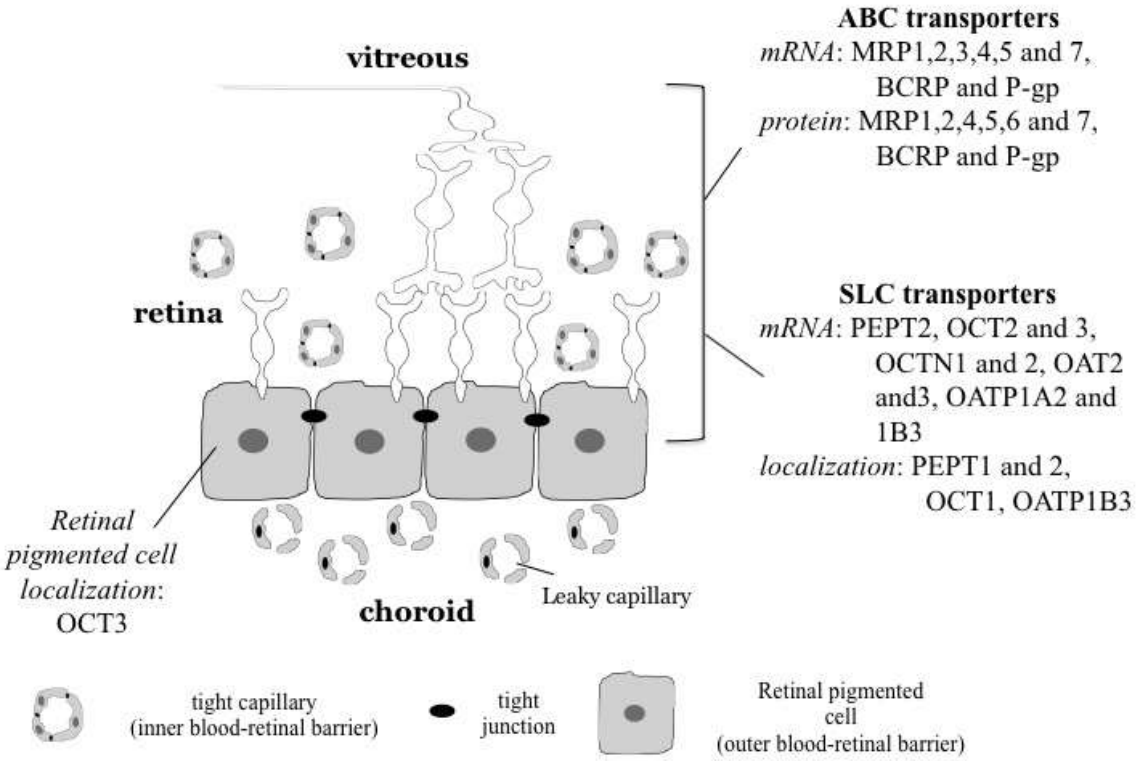

Figure 1.4. Current understanding of drug transporter expression in human retina. mRNAs were detected by RT-PCR and/or qPCR. Proteins were detected by immunoblotting. Localization was done using immunohistochemistry. References are given in the text.

CHAPTER 2: MATERIALS AND METHODS

2.1 Reagents and Antibodies

The mouse anti-α1 subunit of Na,K-ATPase monoclonal antibody (clone M8-P1-A3) was from Thermo Scientific (Rockford, IL, USA). The mouse anti-connexin 43 monoclonal antibody (clone CX-1B1) was from Life Technologies (Burlington, ON, Canada). The rat anti-MRP4 monoclonal antibody (clone M4I-10) used for immunoblotting was from Abcam (Toronto, ON, Canada) – this antibody did not work in immunohistochemistry with paraffin embedded tissues (data not shown), so we used a different antibody for this application. The rabbit anti-MRP4 antibody used in immunohistochemistry was a generous gift from Dr. Frans G. Russel (Radboud University, Nijmegen Medical Centre, the Netherlands). Details of its synthesis and use in immunolocalizing MRP4 to apical membranes of human proximal tubule can be found in a publication by Van et al., (van Aubel et al., 2002). The rabbit anti-OAT1 antibody was from Genway Biotech, Inc (San Diego, CA, USA). The rabbit anti-OAT3 antibody was from Cosmo Bio Co. LTD (Tokyo, Japan). The mouse anti-NaDC3 monoclonal antibody (clone 3A6) was from Abnova (Taipei City, Taiwan). The AlexaFluor 488 goat anti-rabbit, AlexFluor 488 goat anti-mouse, horseradish peroxidase (HRP)-conjugated goat anti-rabbit, HRP-conjugated goat anti-mouse and HRP-conjugated goat anti-rat antibodies were from Life Technologies. Normal goat serum (10% solution) and propidium iodide solution (1 mg/ml) were from Life Technologies. The bicinchoninic acid protein assay kit was from ThermoScientific. The QuantiTect Reverse Transcription

kit and RNeasy mini kit were from Qiagen (Valencia, CA, USA). Custom oligonucleotide primers were synthesized by Integrated DNA Technologies (Coralville, IA, USA). [^{3}H]PAH (40 – 60 Ci/mmol) and [^{3}H]estrone-3-sulfate (50 Ci/mmol) were from American Radiochemicals (St. Louis, MO, USA). [^{3}H]cidofovir (25 Ci/mmol) was from Moravek Biochemicals (Brea, CA, USA). Unless noted otherwise, all other reagents and chemicals were from Sigma-Aldrich (Oakville, ON, Canada).

2.2 Human Tissues

Human cadaver eyes obtained from the National Disease Resource Interchange (Philadelphia, PA, USA) were used for immunohistochemistry and microarray analysis. Human cadaver eyes from four donors used for reverse transcription polymerase chain reaction (RT-PCR) and immunoblotting were obtained from the Capital Health Tissue Bank (Halifax, NS, Canada). All donors were male (Age ranges 19-60 years old) and died of traumatic events. All human eyes were processed within <24 h post enucleation. For RT-PCR and immunoblotting the ciliary processes, retina, retinal pigmented epithelium, iris and cornea were dissected under a microscope and stored in liquid nitrogen until further analysis. Human kidney cortex from a single donor was obtained from the *Eunice Kennedy Shriver* National Institute of Child Health and Human Development (NICHD) Brain and Tissue Bank at the University of Maryland (Baltimore, MD, USA). The use of human cadaver eyes was approved by the Research Ethics Board of Dalhousie University and the Human Subjects Committee of Yale University. The use of human kidney tissue was approved by the Research Ethics Board of Dalhousie

University. Use of the human cadaver eyes and kidney followed the tenets of the Declaration of Helsinki.

2.3 Animal Tissues

Bovine eyes were obtained from W.G. Oulton's & Sons Ltd. (Windsor, NS, Canada) and used within 2 hours of enucleation. Use of the bovine eyes was approved by the Dalhousie University Committee on Laboratory Animals.

2.4 RNA Isolation, RT-PCR and Microarray Analysis

Total RNA was isolated using the RNeasy mini kit according to the manufacturer's instructions. RNA concentration and purity (260/280 ratio) was determined using a Take3 Micro-Volume Plate (2x8 microspots) with an Epoch Microplate Spectrophotometer running Gen5 1.09 Microplate Data Collection and Analysis Software (BioTek Instruments, Inc.). The 260/280 ratios for all samples were between 2.0 and 2.2. One-tenth of a microgram of total RNA was reverse transcribed using the QuantiTect Reverse Transcription kit according to the manufacturer's protocol. The protocol included a step to remove genomic DNA. Sixty nanograms of cDNA were used in the PCR reactions. The oligonucleotide primer sequences used are shown in **Table 2.1**. The PCR components were assembled followed by a single denaturation step for 2 min at 94°C. This was followed by 35 cycles of: 94°C for 30 sec, 55°C for 30 sec and 72°C for 2 min. A final elongation step of 7 min (72°C) was included after the last cycle. Products were separated on 1% agarose gels and visualized with ethidium

bromide. Images of the amplification signals were taken with Kodak EDAS 290 Gel Documentation and Analysis System. Whole-genome expression profiling was done using the Illumina BeadChip array platform (HumanHT-12 v4.0 Expression BeadChip Kit). cRNA labeling and hybridization to the chip and array data analysis were carried out by the Yale Neuroscience Microarray Center (NIH Neuroscience Microarray Consortium) at the Keck Foundation at Yale University.

2.5 SDS-PAGE and Immunoblotting

Crude homogenates of human ciliary body or human renal cortex were prepared by homogenizing ~0.3 g of tissue using a TissueRuptor (Qiagen) in ~1 ml of ice-cold homogenization buffer containing 300 mM sucrose, 1 mM ethylenediaminetetraacetic acid and protease inhibitors (in μM: 4-(2-aminoethyl)benzenesulfonyl fluoride hydrochloride, 104; aprotinin, 0.08; leupeptin, 2; bestatin, 4; pepstatin A, 1.5; E-64, 1.4). The final concentration of crude membrane protein was 2 – 5 μg/ml as determined by the bicinchoninic protein assay method. The crude membrane protein was diluted with an equal volume of 2× Laemmli sample buffer containing 2.5% β-mercaptoethanol (final concentration). Except for immunodetection of MRP4, all samples were heated to 100°C for 5 minutes. Twenty micrograms of protein were separated on 4-12% Tris-glycine polyacrylamide gels and transferred to polyvinylidine membranes. The membranes were blocked for 1 h at room temperature in phosphate buffered saline (PBS) containing 0.05% Tween-20 (PBS-T) and 5% non-fat dry milk (blocking buffer). The membranes were incubated overnight at 4°C in primary antibody diluted in blocking buffer. The final

concentration of the primary antibodies are as follows: rabbit anti-OAT1 (5 μg/ml), rabbit anti-OAT3 (1 μg/ml), rat anti-MRP4 (1.5 μg/ml) and mouse anti-NaDC3 (0.5 μg/ml). **Table 2.2** summarizes primary antibodies and concentrations used for immunoblotting. After extensive washing in PBS-T the membranes were incubated for 1 h at room temperature with secondary antibodies diluted in blocking buffer (final concentration of 0.4 μg/ml). After extensive washing in PBS-T the membranes were incubated in SuperSignal West Femto chemiluminescent substrate (ThermoScientific) according to the manufacturer's protocol. Immunoreactivity was detected on CL-XPosure film (ThermoScientific) using a Konika Minolta SRK-101A processor.

2.6 Immunohistochemistry

The human cadaver eye was fixed overnight at 4°C in periodate-lysine-paraformaldehyde fixative containing in (mM): 75 L-lysine, 10 sodium periodate, 37 Na_2HPO_4, pH 7.4, and 2% paraformaldehyde. After fixation the eye was equilibrated in 70% ethanol, embedded in paraffin, and 5 μm sections were cut and placed on glass slides. All subsequent immunohistochemistry procedures used gentle shaking on an orbital shaker in a humidified atmosphere. Following paraffin removal and rehydration the specimens were blocked for 1 h at room temperature in 10% normal goat serum. After blocking, the specimens were incubated overnight at 4°C with primary antibody diluted in 10% normal goat serum. The concentration of primary antibodies used for immunohistochemistry are as follows: rabbit anti-MRP4 (1:500 dilution; protein concentration unknown), mouse anti-connexin 43 (6.75 μg/ml), mouse anti-Na,K-ATPase

(7.28 μg/ml), rabbit anti-OAT1 (1 μg/ml) and rabbit anti-OAT3 (5 μg/ml). Primary antibodies and concentrations used for immunohistochemistry are listed in **Table 2.2**. After extensive washing with PBS the specimens were incubated for 1h at room temperature with Alexa 488-conjugated secondary antibodies diluted in 10% normal goat serum (final concentration of 4 – 10 μg/ml). Omission of secondary antibodies served as negative controls and resulted in a near undetectable level of fluorescence (not shown). Following extensive washing with PBS the specimens were incubated for 5 min with PBS containing propidium iodide (5 μg/ml) to label nuclei. Following several washes with PBS immunoreactivity was visualized using a Zeiss LSM 510 META laser scanning confocal microscope at the Cellular and Molecular Digital Imaging facility in the Faculty of Medicine at Dalhousie University.

2.7 Ussing Chamber Experiments

Following dissection bovine ciliary body was mounted in Ussing chambers with an aperture size of 0.12 cm^2. Tissues were mounted in that only pars plicata was placed over the aperture. Each hemichamber contained 1.2 ml of Kreb's solution containing: 117 mM NaCl, 4.6 mM KCl, 20 mM $NaHCO_3$, 6 glucose, 1 mM $MgCl_2$, 1.5 mM $CaCl_2$ and 10 mM hydroxyethyl piperazineethanesulfonic acid (HEPES), pH 7.4. The buffer inside the chambers was continuously stirred with magnetic stir bars, gassed with 95% O_2/5% CO_2, and the temperature was maintained at 37°C with water circulated on the outside surface of the chambers. Ag/AgCl electrodes were used to monitor transepithelial potential difference (TPD) and as short-circuiting electrodes. The Ag/AgCl electrodes

were connected to the aqueous humor and blood sides of the tissue with agar bridges (3 M KCl-2% agar). Electrode asymmetry was corrected at the beginning and end of each experiment with fluid resistance compensation. Transepithelial resistance (TER) was determined by the change in TPD generated by a brief 10-μA pulse controlled by a high-impedance automatic dual voltage clamps (DVC 4000; World Precision Instruments, Sarasota, FL). Transepithelial electrical data was collected and analyzed using a PowerLab 28T and LabChart software, respectively (ADInstruments, Colorado Springs, CO, USA).

All transport experiments were conducted under voltage-clamped conditions, i.e., in the absence of electrical and chemical gradients. Thus, any net movement of compound across the tissue was due to active transport, that is, only the net transport is the true measure of active transport. The unidirectional fluxes could be a combination of both passive and active transport. Flux measurements began following the addition of a tracer level (~20 – 50 nM) of [^{3}H]labeled compound (PAH, estrone-3-sulfate or cidofovir) to the appropriate hemichamber (aqueous humor side or blood side) along with a higher concentration of unlabeled compound (5 μM, 15 μM or 1 mM final concentration – as stated in the Figure Legends) added to both hemichambers. In some cases, inhibitor drug (probenecid or novobiocin, 100 μM final concentration) was added to the aqueous humor side of the tissue. Ten microliter samples (in duplicate) were taken from the labeled side at the beginning and end of each experiment. Duplicate 50-μl samples were collected from the unlabeled side and replaced with 100 μl of unlabeled solution at 30-min intervals over a period of 2 h. Radioactivity content in the samples was determined by liquid scintillation spectroscopy (LS6500, Beckman Coulter). The

difference between the unidirectional aqueous humor-to-blood and blood-to-aqueous humor fluxes represents net active flux. For an individual replicate, control and transport protein inhibitor treated tissues were prepared from the same ciliary body and the flux measurements were performed simultaneously. TPD and TER were determined at the beginning and end of each experiment to monitor tissue viability. A brief overview of this technique is found in **Figure 2.1**, where an individual Ussing chamber set-up and the entire system are displayed in Figure 2.1A and Figure 2.1B, respectively, and the experimental design is in Figure 2.1C.

2.8 Statistics

Experimental results are presented as mean ± standard error of the mean. Comparison of sample means was done using an unpaired student's t-test. All statistical analysis was performed with GraphPad Prism (version 5) and deemed significant when $p < 0.05$.

Table 2.1. Oligonucleotide sequence of primers used for RT-PCR

Species	Transporter	Oligonucleotide primer
Human	OAT1	sense strand: 5′-TCATCTTGAACTACCTGCAGAC-3′ antisense strand: 5′-CAGAGTCCATTCTTCTCTTGTG-3′
	OAT3	sense strand: 5′-CTTCGTCTTCTTCCTATCATCC-3′ antisense strand: 5′-AGACCTAGGGACAGAGAGCTAAG-3′
	NaDC3	sense strand: 5′-AGTACTTCCTCGACACCAACTT-3′ antisense strand: 5′-AGTCAAACCACCACTTGAGAG-3′
	MRP4	sense strand: 5′-ATCTGCTGTCCAATGATGTG-3′ antisense strand: 5′-CAGTTCGAACAAGTGTCTGC-3′
Bovine	Oat1	sense strand: 5′-AGCTGGCTCAGTCCTTATACAT-3′ antisense strand: 5′-GACAGCACCGTAGATAAAGAGAG-3′
	Oat3	sense strand: 5′-ACAACCTGCTACAGATCTTCAC-3′ antisense strand: 5′-GATAGCTTATGGCCAGTGTAGTG-3′
	Nadc3	sense strand: 5′-AGTACTTCCTGGACACCAACTT-3′ antisense strand: 5′-GTCTCTGTGTTGGGAGCTTTA-3′
	Mrp4	sense strand: 5′-GATGACATGTACTCGGTGTTTC-3′ antisense strand: 5′-CTGTAATCAGGTTGTCAAGGAG-3′

Table 2.2. Primary antibodies and concentrations used for immunoblotting and immunohistochemistry (IHC).

Application	Primary Antibody	Final Concentration	Source
Immunoblotting	Rabbit anti-OAT1	5 µg/ml	Genway Biotech, Inc
	Rabbit anti-OAT3	1 µg/ml	Cosmo Bio Co. LTD
	Rat anti-MRP4	1.5 µg/ml	Abcam
	Mouse anti-NaDC3	0.5 µg/ml	Abnova
IHC	Rabbit anti-MRP4	Unknown, 1:500 dilution	Gift from Dr. Frans G. Russel
	Mouse anti-connexin 43	6.75 µg/ml	Life Technologies
	Mouse anti-Na,K-ATPase	7.28 µg/ml	Thermo Scientific
	Rabbit anti-OAT1	1 µg/ml	Genway Biotech, Inc
	Rabbit anti-OAT3	5 µg/ml	Cosmo Bio Co. LTD

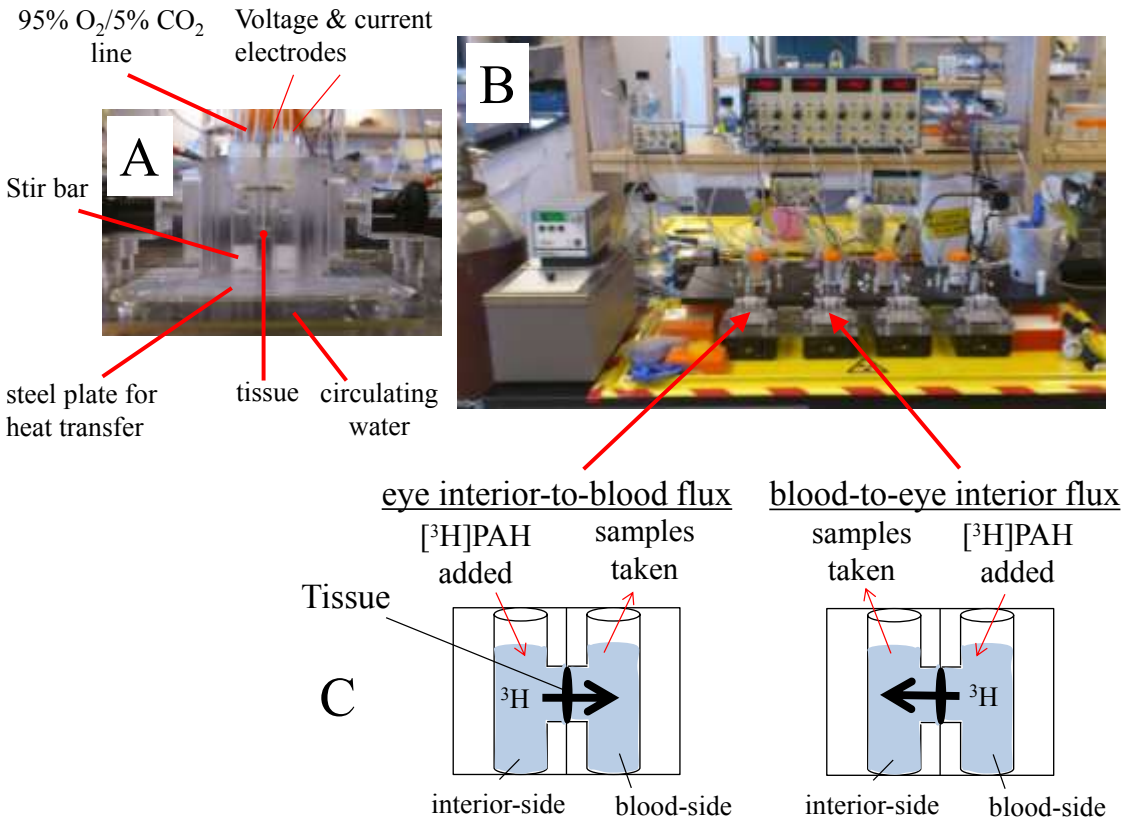

Figure 2.1. Ussing chamber methodology. Unidirectional and net active transepithelial flux of *para*-aminohippurate (PAH) was determined using bovine ciliary body in Ussing chambers. Panel A and Panel B show an individual Ussing chamber and the entire system, respectively. Panel C shows how the unidirectional fluxes are measured. Net flux is the difference between the unidirectional fluxes.

CHAPTER 3: RESULTS

3.1 mRNA Expression of Organic Anion Transporters in Ocular Tissues

Expression of 33 genes corresponding to the major OA drug transporters in the SLC and ABC transporter families was determined by microarray in the following microdissected ocular tissues: cornea, trabecular meshwork, iris, lens epithelium, ciliary body, retina and retinal pigmented epithelium (**Figure 3.1**). The transporters examined were the organic anion transporters (OATs), urate transporter 1 (URAT1), Na-phosphate transporters (NPTs), Na-dicarboxylate cotransporters (NaDCs), multidrug resistance-associated proteins (MRPs), breast cancer resistant protein (BCRP), P-glycoprotein (P-gp) and the organic anion transporting polypeptides (OATPs). We further focused on the expression of OAT1, OAT3, NaDC1, NaDC3 and MRP4 in the ciliary body since the microarray data suggested all five transporters are present, they are primary components of the renal OA transport system (Pelis and Wright, 2011), and previous in vivo and in vitro functional studies showed OA transport activity consistent with their expression in the ciliary body (see Chapter 1).

RT-PCR was further used to examine the mRNA expression of OA transporters (MRP4, NaDC1, NaDC3, OAT1 and OAT3) in the ciliary body, retina, iris, retinal pigmented epithelium and cornea. All of the tissues examined expressed the α1 subunit of Na,K-ATPase, MRP4 and NaDC3, whereas the other proteins were differentially expressed (**Figure 3.2**). NaDC1 mRNA was only detected in the retina, OAT1 mRNA in the ciliary body, iris and retinal pigmented epithelium, and OAT3 mRNA in the ciliary

body and to a lesser extent in the retinal pigmented epithelium. The observation that the ciliary body expressed most of the members of the renal OA transport system led us to focus further on this tissue.

3.2 Determination of Active Transepithelial PAH Transport Across Ciliary Body

PAH is a well-established substrate of the renal OA transport system. To determine if the ciliary body supports active PAH transport we measured the transepithelial transport of PAH under short-circuited conditions across the freshly dissected bovine ciliary body in Ussing chambers. **Figure 3.3A** shows a representative flux experiment with 1 mM PAH bathing both sides of the tissue. The unidirectional aqueous humor-to-blood flux was greater than the blood-to-aqueous humor flux, with net active transport in the aqueous humor-to-blood direction – net active transport approached steady-state at the 2 h time point. In several different experiments the aqueous humor-to-blood flux was 5.3-fold higher at t = 2h than the blood-to-aqueous humor flux (**Figure 3.3B**). The TER, TPD and I_{sc} values for these control experiments were 66.8 ± 5.9 $\Omega \cdot cm^2$, -0.32 ± 0.2 mV (aqueous humor side negative) and -19.9 ± 4.2 $\mu A \cdot cm^{-2}$, respectively. The transepithelial electrical properties determined here are in relatively good agreement with previous results (To et al., 1998). We also examined PAH transport at a bath concentration of 5 μM. Under these conditions the aqueous humor-to-blood flux (1.05 ± 0.08 nmoles $\cdot$ cm^{-2} $\cdot$ h^{-1}) was 11.7-fold higher than the blood-to-aqueous humor flux (0.09 ± 0.02 nmoles $\cdot$ cm^{-2} $\cdot$ h^{-1}) at t = 2h (n = 3, $P < 0.001$, two-tailed unpaired students *t*-test). Similar to the human ciliary body, mRNA for Oat1, Oat3,

Nadc3 and Mrp4 were detected in bovine ciliary body extracts by RT-PCR (**Figure 3.3C**).

3.3 Inhibition of Transepithelial PAH Transport Across Ciliary Body

Given the evidence for active PAH transport across the bovine ciliary body, we also performed inhibition experiments using the well-known renal OA transport inhibitors, probenecid and novobiocin. The inhibitors were added to the aqueous humor side of the tissue only since we speculated that at least OAT1, which transports PAH, and is inhibited by probenecid (Ingraham et al., 2014) and novobiocin (Duan and You, 2009), is located in basolateral membranes of non-pigmented epithelial cells. We used a bath PAH concentration of 1 mM given that net transport approached steady-state under these conditions, but did not when the bath contained 5 μM PAH (not shown). Probenecid nearly abolished all net active transport by reducing the aqueous humor-to-blood flux (**Figure 3.4**). Novobiocin completely inhibited net active secretion, but its effect was due to an apparent simultaneous reduction in the aqueous humor-to-blood flux and an increase in the blood-to-aqueous humor flux (**Figure 3.5**). Neither inhibitor influenced the transepithelial electrical properties (not shown).

3.4 Investigation of Active Estrone-3-sulfate and Cidofovir Transport Across Ciliary Body

Since PAH is a preferential substrate of OAT1 versus OAT3(Zhang et al., 2004), and both the human and bovine ciliary body express OAT3, the transepithelial transport of estrone-3-sulfate (a preferential substrate of OAT3; (Zhang et al., 2004)) across the bovine ciliary body in Ussing chambers was examined. We also examined the transport of cidofovir since it is used clinically to treat AIDS-associated cytomegalovirus and is an OAT1 substrate (Cihlar et al., 1999). At a bath concentration of 5 μM the estrone-3-sulfate aqueous humor-to-blood flux (26.1 ± 7.3 nmoles · cm^{-2} · h^{-1}) was 3.5-fold higher than the blood-to-aqueous humor flux (7.45 ± 1.5 nmoles · cm^{-2} · h^{-1}) at t = 2h (**Figure 3.6)**. Interestingly, there was no significant difference in the unidirectional fluxes of cidofovir across the bovine ciliary body (**Figure 3.6**).

3.5 Expression of Organic Anion Transporters in the Ciliary Body

RT-PCR and immunoblotting for OAT1, OAT3, MRP4 and NaDC3 was conducted for additional evidence for their expression in human ciliary body using preparations from four separate human donors – human renal cortex was used as a positive control in each case. mRNA transcripts for OAT1, OAT3, MRP4 and NaDC3 were detected in all human donor samples and in human kidney (**Figure 3.7**).

Furthermore, mRNA transcripts for additional transporters, including PEPT2, OCT2 and MPR5, were also detected by RT-PCR (**Figure 3.7)**. MRP5 was examined since it was detected in the microarray analysis **(Figure 3.1).** PEPT2 and OCT2 were also detected by microarray analysis (data not shown in **Figure 3.1**). All of the amplified products were of the expected size based on the oligonucleotides primers used and their respective sequences.

Protein for OAT1, OAT3, MRP4 and NaDC3 were also detected in ciliary body of all donors examined, as well as in human renal cortex (**Figure 3.8**). OAT1, OAT3, MRP4 and NaDC3 migrated on the SDS-PAGE gels with apparent sizes of ~60 kDa, ~60 kDa, ~160 kDa and ~55 kDa, respectively. There were apparent differences in the expression level of the various transport proteins between donors and with respect to the kidney tissue – equal amounts of crude membrane protein were loaded into each lane (20 μg). Overall, the expression of the transporters in the ciliary body samples was slightly lower or equivalent to that found in the kidney. The expression level of OAT1, MRP4 and NaDC3 were lower in donors one and three, but OAT3 expression was highest in these donors.

3.6 Cellular and Subcellular Localization of Organic Anion Transporters in Ciliary Body

Immunohistochemistry was used to determine the cellular and subcellular expression pattern of OAT1, OAT3, MRP4 and NaDC3 in paraffin embedded sections of human eye (**Figure 3.9**). The α1 subunit of Na,K-ATPase was used as a marker of

basolateral membranes of pigmented cells and non-pigmented epithelium while connexin 43 was used as a marker of apical membranes of pigmented cells and non-pigmented epithelium. The level of immunoreactivity for Na,K-ATPase was high in the basolateral membrane of non-pigmented cells and much weaker (almost undetectable) at the basolateral membrane of pigmented cells. Connexin 43 had a punctate staining pattern that was sporadic and occurred at the apical junction of pigmented and non-pigmented cells. The pattern of Na,K-ATPase and connexin 43 immunoreactivity in the ciliary body is consistent with previous reports (Flugel and Lutjen-Drecoll, 1988;Shahidullah and Delamere, 2014). The level of OAT1 was relatively weak, but appeared to occur predominately in the non-pigmented epithelial cells with an expression pattern consistent with its occurrence in basolateral membranes. OAT3 also appeared to localize to basolateral membranes of non-pigmented epithelial cells. In contrast, MRP4 had a localization pattern consistent with its expression in basolateral membrane of pigmented cells. Attempts to immunolocalize NaDC3 to human ciliary body were unsuccessful.

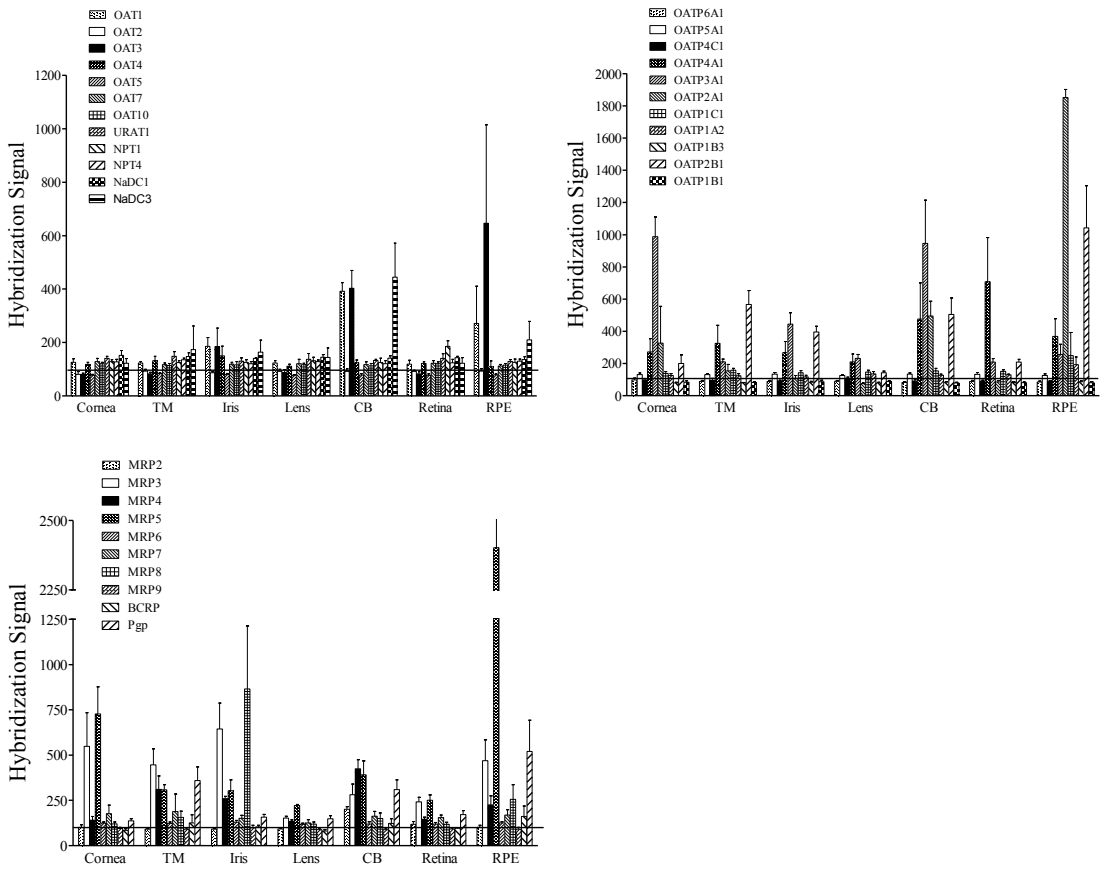

Figure 3.1. Microarray analysis of OA transporter expression in microdissected human ocular tissues. The data are mean ± the standard error of the mean of the hybridization signal from tissue from 5-6 individual human donor eyes. The horizontal line represents a background level of hybridization signal, i.e., only values above this line are considered a positive signal. TM, trabecular meshwork; CB, ciliary body; RPE, retinal pigmented epithelium. URAT1, urate transporter 1; NPT, Na-phosphate transporter; OATP, organic anion transporting polypeptide; BCRP, breast cancer resistant protein; P-gp, P-glycoprotein.

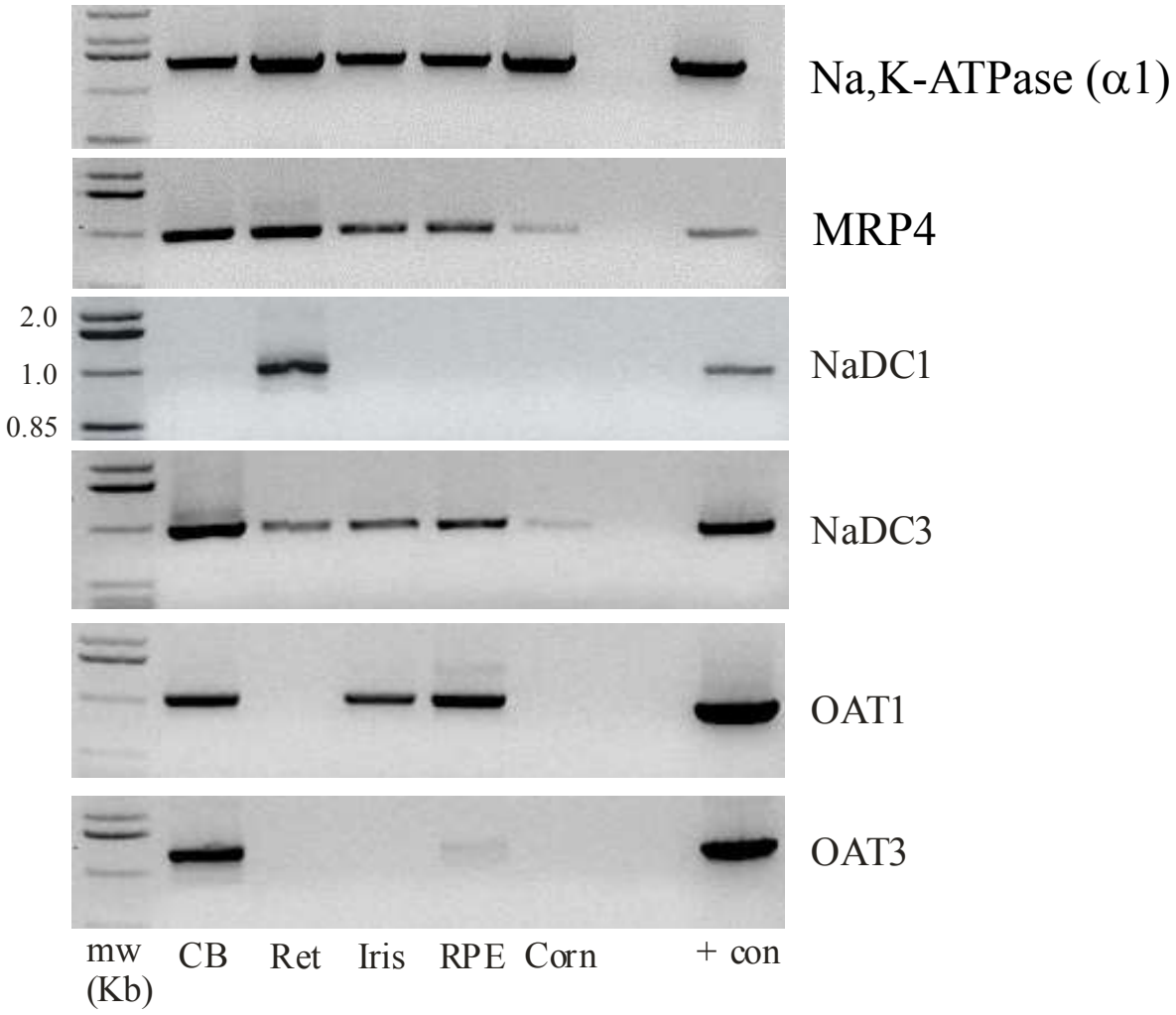

Figure 3.2. mRNA expression of organic anion transporters common to kidney in human ocular tissues. RT-PCR analysis of Na,K-ATPase (α1 subunit), MRP4, NaDC1, NaDC3, OAT1 and OAT3 in human ciliary body (CB), retina (Ret), iris, retinal pigmented epithelium (RPE) and cornea (Corn). Kidney was used as a positive control. PCR products were separated on 1% agarose gels and visualized with ethidium bromide.

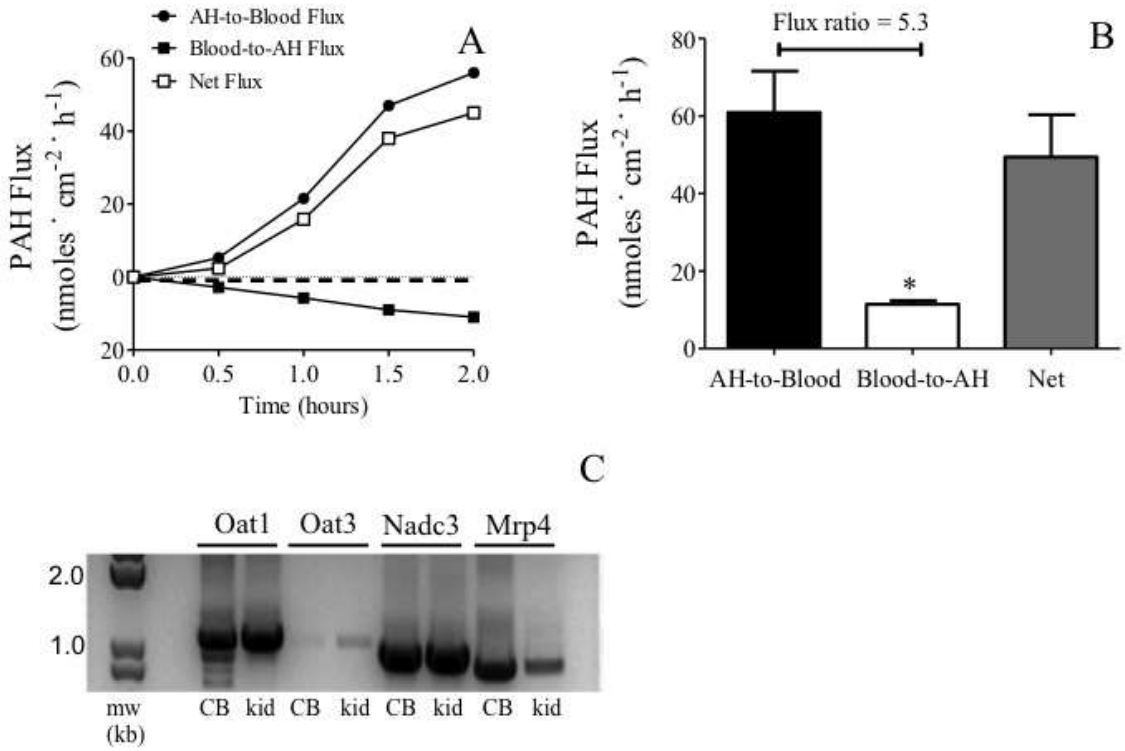

Figure 3.3. Bovine ciliary body supports net active transport of PAH in the aqueous humor-to-blood direction. Unidirectional fluxes (aqueous humor-to-blood, AH-to-blood; blood-to-aqueous humor, blood-to-AH) and net active flux of PAH across bovine ciliary body in Ussing chambers (Panel A and B). Panel A is a representative time-course experiment (n = 1). Panel B are the fluxes at steady-state (t = 2h) from 4 separate experiments (mean ± standard error of the mean). The unlabeled concentration of PAH used was 1 mM. Net flux is the difference between the unidirectional fluxes and is in the aqueous humor-to-blood direction. *P < 0.05, significantly different from the AH-to-blood flux, two-tailed unpaired student's *t*-test. Panel C is mRNA expression analysis of Oat1, Oat3, Nadc3 and Mrp4 in bovine ciliary body (CB) by RT-PCR. Kidney was used as a positive control (kid). PCR products were separated on 1% agarose gels and visualized with ethidium bromide.

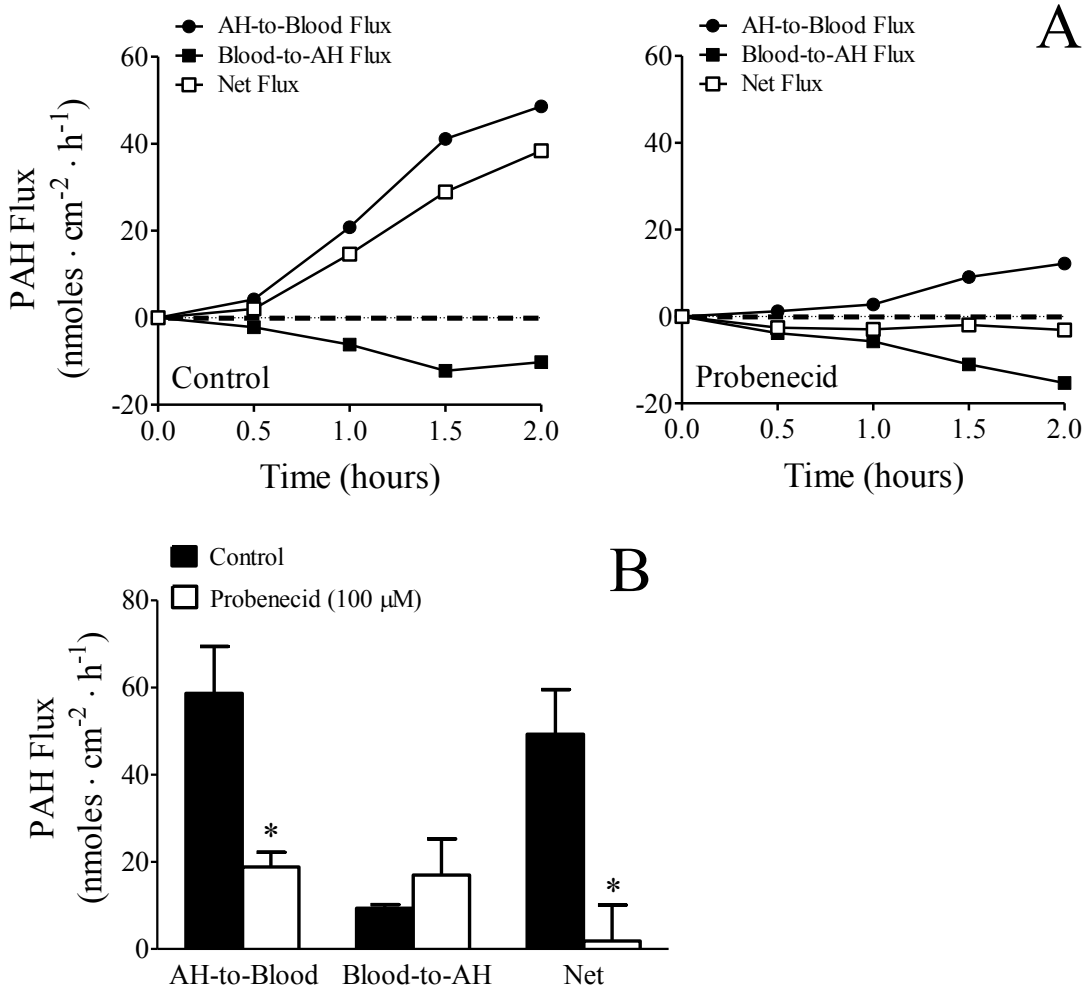

Figure 3.4. Transepithelial transport of PAH across the bovine ciliary body in Ussing chambers is inhibited by probenecid. Panel A are representative fluxes in the absence or presence of 100 μM probenecid added to the aqueous humor side of the tissue only. Panel B is the mean ± SEM of the fluxes at t = 2h from three separate experiments. The concentration of unlabeled PAH was 1 mM. *P < 0.05, significantly different from control, two-tailed unpaired student's *t*-test.

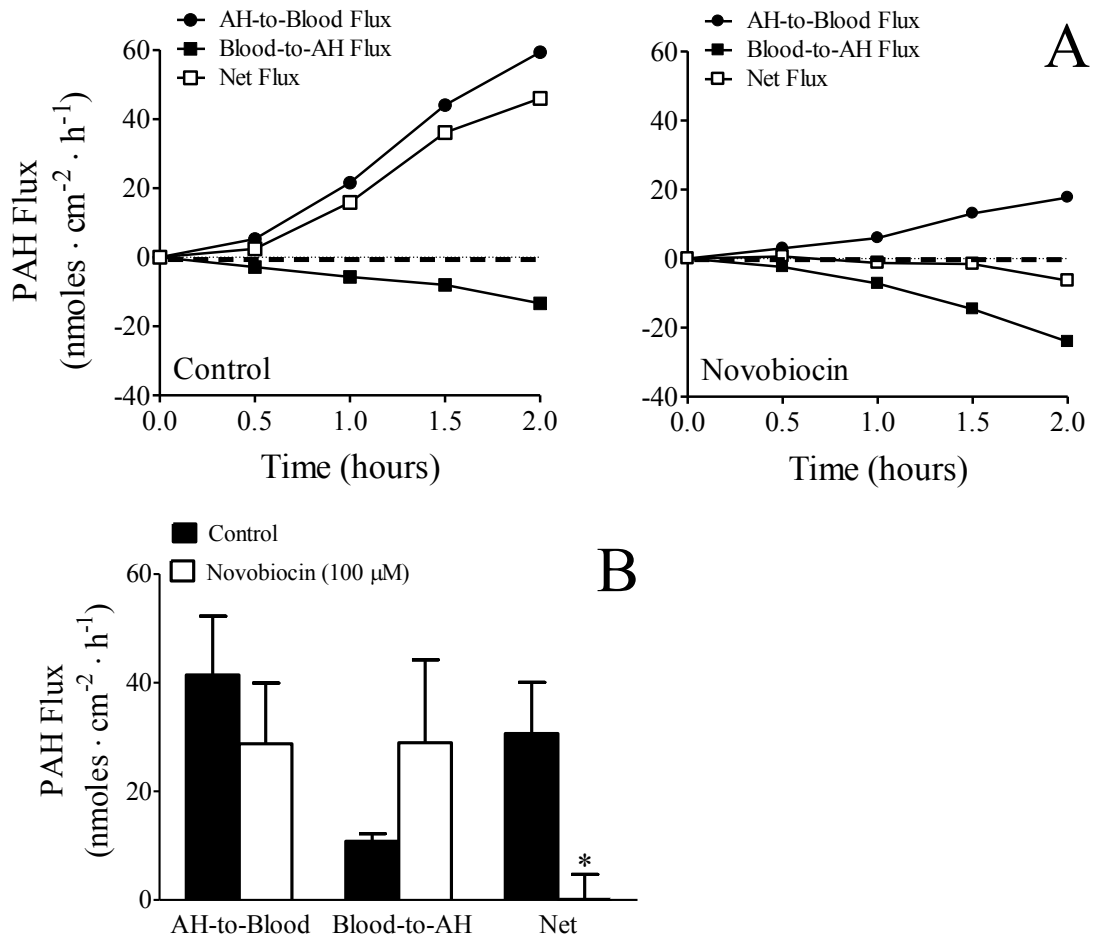

Figure 3.5. Transepithelial transport of PAH across the bovine ciliary body in Ussing chambers is inhibited by novobiocin. Panel A are representative fluxes in the absence or presence of 100 μM novobiocin added to the aqueous humor side of the tissue only. Panel B is the mean ± SEM of the fluxes at t = 2h from three separate experiments. The concentration of unlabeled PAH was 1 mM. *P < 0.05, significantly different from control, two-tailed unpaired student's *t*-test.

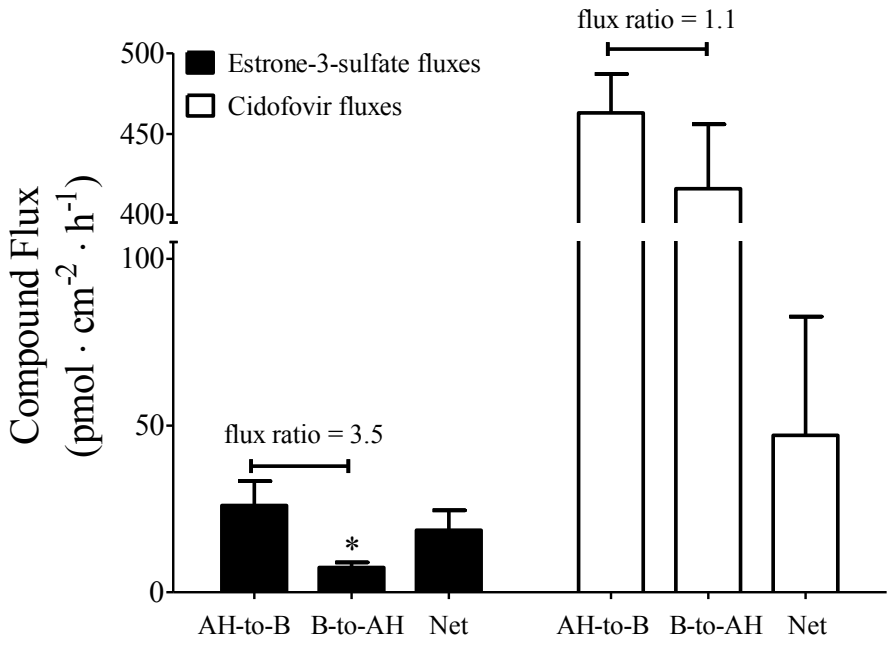

Figure 3.6. Transepithelial transport of estrone-3-sulfate and cidofovir. Unidirectional fluxes (aqueous humor-to-blood, AH-to-B; blood-to-aqueous humor, B-to-AH) and net active flux of estrone-3-sulfate or cidofovir across bovine ciliary body in Ussing chambers. The flux values were obtained at t = 2h and are the mean ± standard error of the mean of 4 (estrone-3-sulfate) or 3 (cidofovir) separate experiments. The unlabeled concentration of estrone-3-sulfate and cidofovir was 5 μM. Net flux is the difference between the unidirectional fluxes. *P < 0.05, significantly different from the AH-to-blood flux, two-tailed unpaired student's *t*-test.

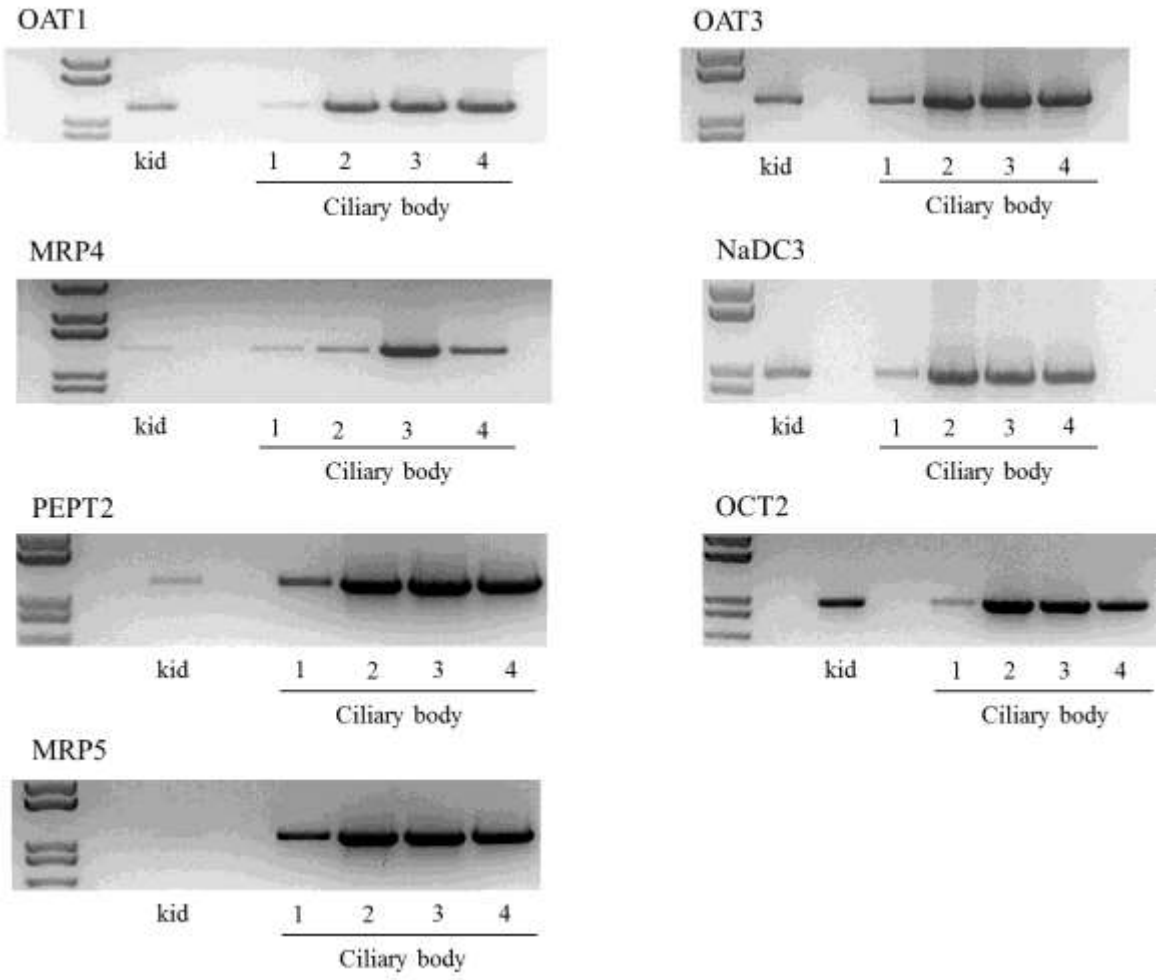

Figure 3.7. mRNA expression of SLC transporters in the ciliary body from four separate human donors. RT-PCR analysis showing OAT1, OAT3, MRP4, NaDC3, PEPT2, OCT2 and MRP5 mRNA transcripts in the ciliary body from four separate human donors (1-4). Human kidney cortex was used as a positive control (kid). PCR products were separated on 1% agarose gels and visualized with ethidium bromide.

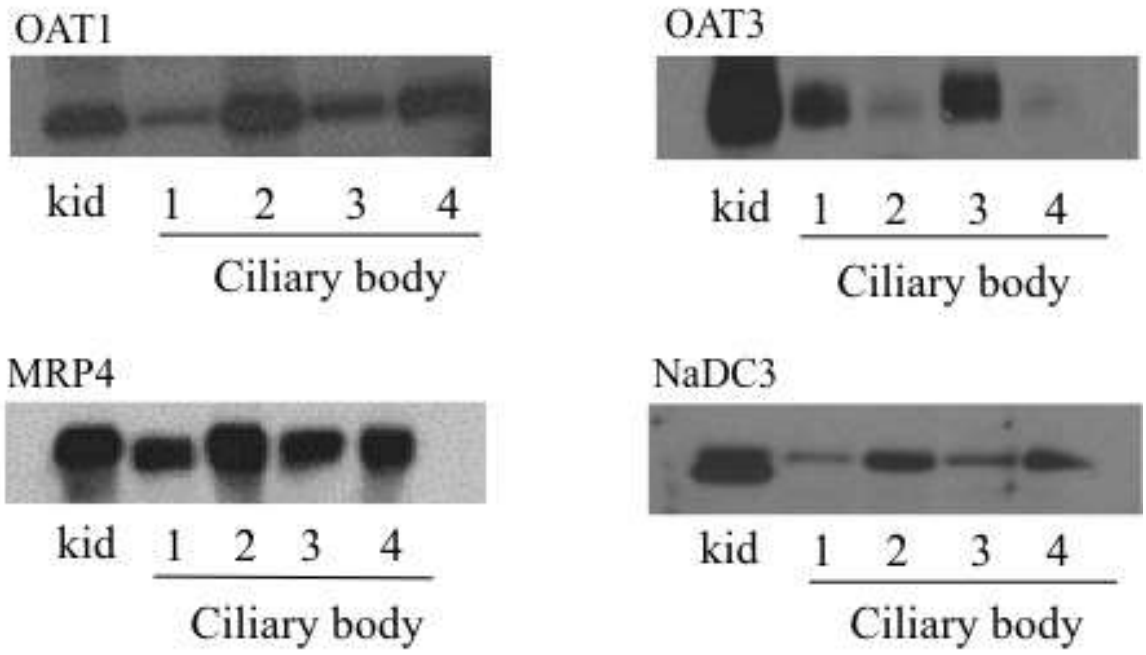

Figure 3.8. Protein expression of organic anion transporters common to kidney in the ciliary body of four separate human donors. Immunoblot showing the expression of OAT1, OAT3 and MRP4 in the human ciliary body of four different donors (1-4). Crude homogenate of human kidney cortex served as a positive control (kid). Twenty micrograms of crude homogenate from each of the tissue samples was separated on 4 – 12 % SDS-PAGE gels before electrophoretic transfer of the proteins to polyvinylidene difluoride membranes. Immunoreactivity was detected using protein specific antibodies and enhanced chemiluminescence detection.

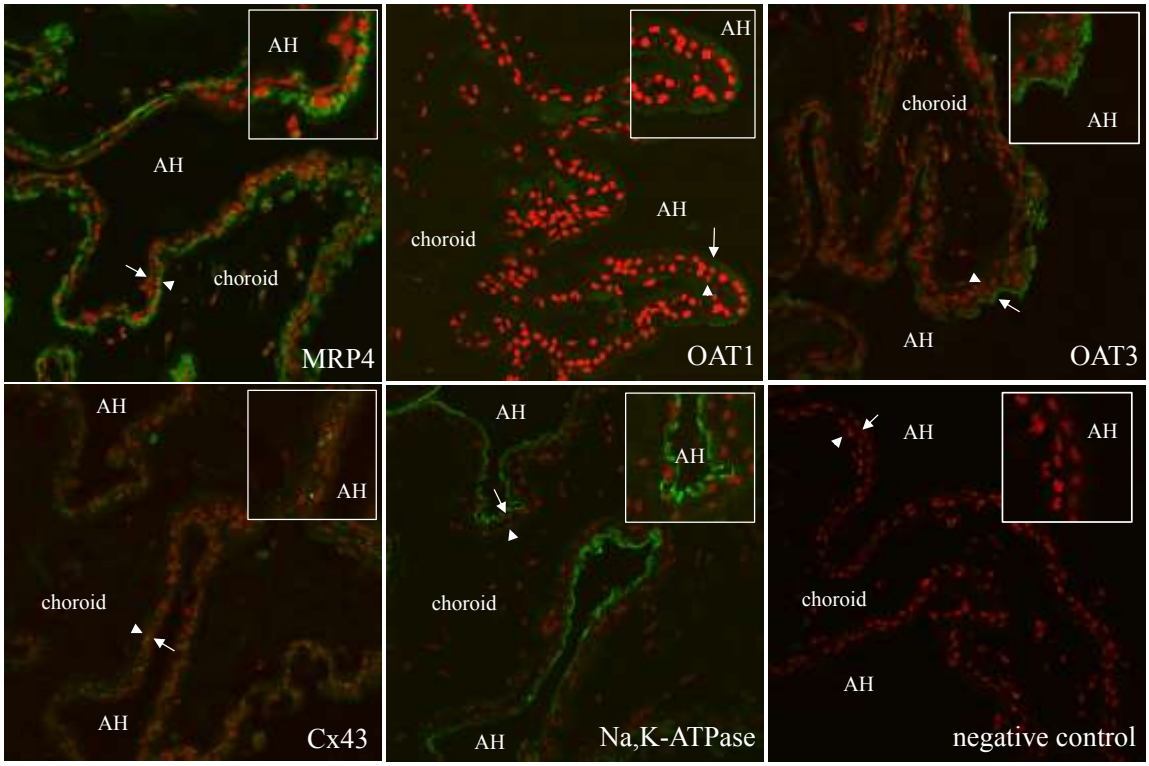

Figure 3.9. Cellular and subcellular distribution of organic anion transporters in the human ciliary body. Immunolocalization of Na,K-ATPase, connexin 43 (Cx43), MRP4, OAT1 and OAT3 in paraffin embedded human eye. Na,K-ATPase was used as a marker of basolateral membranes of pigmented and non-pigmented cells. Connexin 43 (Cx43) was used as a marker for the apical membrane of both cell types. Proteins of interest are in green and nuclei are stained red with propidium iodide. The arrowheads point to pigmented cells whereas the arrows point to non-pigmented cells. The inset figures are magnifications of the areas near the arrow and arrowhead. AH = aqueous humor. Limited immunoreactivity was detected when the primary antibody was omitted (negative control).

CHAPTER 4: DISCUSSION

4.1 Overview

Intraocular tissues are well protected from exposure to xenobiotic agents, including therapeutic drugs, which has led to intensive research into ocular drug delivery strategies. Many drugs used to treat eye diseases are OAs at physiological pH, such as many antibiotics, antivirals, nonsteroidal anti-inflammatory drugs and chemotherapeutics. For many of these OAs, their elimination from plasma is mediated in part by renal proximal tubular secretion involving the concerted activity of OA transporters in basolateral and apical membranes of proximal tubule cells. Notably, OAT1, OAT3 and NaDC3 occur in basolateral membranes and are involved in cellular uptake of OAs, whereas MRP2 and MRP4 are involved in efflux of OAs across apical membranes into the tubular filtrate (Pelis and Wright, 2011).

Most of the currently available data on OA transport in the human eye are based on in vitro studies with excised animal tissues or in vivo studies using intravitreal injection. These studies showed that the accumulation of OAs by the ciliary epithelium is dependent on metabolic energy and temperature, is saturable, and is inhibited by other OAs, including probenecid (Becker, 1960;Sugiki et al., 1961;Bito, 1972). In order to better understand the process of OA transport by the ciliary body we performed molecular and functional studies to identify the OA transporters that possibly contribute to OA transport by the ciliary body.

Previous studies showed that MRP2 is expressed in the apical membrane of non-pigmented epithelial cells and it was proposed that it contributes to cellular efflux of OAs into the choroidal blood (Pelis et al., 2009). In the present study, an initial screen for OAT1, OAT3, NaDC3 and MRP4 in microdissected ocular tissues using microarray and RT-PCR revealed that each occur in the ciliary body, which led to the hypothesis that the tissue would support the transepithelial transport in the aqueous humor-to-blood direction of prototypic substrates of the renal OA transport system.

4.2 Ciliary Body Supports Elimination of Organic Anions from the Eye

To probe for evidence of OA transport across the ciliary body, we initially examined transepithelial transport of PAH, estrone-3-sulfate and cidofovir using bovine ciliary body mounted in Ussing chambers. PAH, estrone-3-sulfate and cidofovir were chosen as substrates since they are all secreted by proximal tubules via the OA transport system (Irish, III and Dantzler, 1976;Shuprisha et al., 1999;Cundy et al., 1995;Lungkaphin et al., 2006). Net PAH transport across the ciliary body in Ussing chambers was in the aqueous humor-to-blood direction, and active (voltage-clamped conditions). Consistent with these results, PAH actively accumulates in in vitro preparations of monkey ciliary body (Stone, 1979). The flux ratio (aqueous humor-to-blood flux/blood-to-aqueous humor flux) was ~2-fold higher at a PAH bath concentration of 5 μM (flux ratio of 11.7) versus 1 mM (flux ratio of 5.3). The decrease in flux ratio with increasing PAH concentration suggests that the rate-limiting step in transepithelial

PAH secretion can be saturated – although it was likely not saturated at the 1 mM concentration, as the flux ratio was >1 under these conditions.

Similar to PAH, the active transport of estrone-3-sulfate across the ciliary body in Ussing chambers was in the aqueous humor-to-blood direction (flux ratio of 3.5). In contrast, there was no active transport of cidofovir, i.e., the aqueous humor-to-blood flux and blood-to-aqueous humor flux were not different from each other. Renal tubular secretion of cidofovir is not particularly robust. That is, the renal clearance (CL_R) of cidofovir exceeds the glomerular filtration rate (GFR), but only by a relatively small fraction ($CL_{R,cidofovir}/GFR \cong 1.5$(Cundy et al., 1995)). Nephrotoxicity is a dose-limiting toxicity for cidofovir in the clinic (Cundy, 1999), largely due to OAT1-mediated uptake of cidofovir into proximal tubule cells (Uwai et al., 2007;Ho et al., 2000), but, perhaps, also due to the slow rate at which cidofovir is effluxed from the cells. MRP2 and MRP4, which localize to apical membranes of proximal tubule, do not support ATP-dependent cidofovir transport (Imaoka et al., 2007). The ciliary epithelium generates aqueous humor, which is necessary for maintenance of intraocular pressure (IOP). Interestingly, an adverse event associated with cidofovir treatment for cytomegalovirus retinitis is low intraocular pressure (ocular hypotony) (Bainbridge et al., 1999). It is possible that OAT1-mediated uptake of cidofovir into ciliary epithelial cells, and its slow rate of cellular efflux, contribute to this adverse event. Probenecid is used to prevent cidofovir-induced nephrotoxicity by blocking OAT1-mediated cidofovir uptake (Cundy, 1999), and may prove useful in ameliorating ocular hypotony in patients receiving cidofovir.

4.3 Transepithelial PAH Transport is Inhibited by Organic Anion Transporter Inhibitors

The effects on transepithelial PAH transport of probenecid and novobiocin were examined since they both inhibit multiple OA transporters. We specifically avoided trying to use selective inhibitors of individual transporters in these experiments since a complete profile of the OA transporters in the ciliary body is unknown, and OA transporters in the SLC and ABC families have a tendency for overlapping ligand selectivity, making it nearly impossible to identify selective inhibitors. Addition of probenecid or novobiocin to the aqueous humor side of the tissue completely abolished net active PAH transport (flux ratio of ~1). Although both drugs were added to the aqueous humor side of the tissue, we cannot rule out the possibility that the drugs entered the cells and inhibited the apical efflux pathway. Probenecid inhibited by reducing the aqueous humor-to-blood flux. Consistent with the effects of probenecid on transepithelial PAH transport, probenecid inhibited PAH accumulation into monkey ciliary body in vitro (Stone, 1979). The effects of novobiocin were more complex – both unidirectional fluxes appeared to change. The apparent increase in the blood-to-aqueous humor flux caused by novobiocin may reflect the ability of the novobiocin gradient, in the aqueous humor-to-blood direction, to reverse PAH transport via anion exchange mechanisms, which are known to occur in apical membranes of proximal tubule (Pelis and Wright, 2011).

4.4 Organic Anion Transporters Are Expressed in the Ciliary Body

The transport activity observed led us to speculate that OAT1, OAT3 and NaDC3 occur in basolateral membranes of non-pigmented cells and MRP4 in either basolateral membranes of pigmented cells, or, localizes to apical membranes of non-pigmented cells along with MRP2 (Pelis et al., 2009). mRNA (RT-PCR) and protein (immunoblotting) expression for OAT1, OAT3, NaDC3 and MRP4 were examined in multiple human donors. mRNA and protein for each transporter was expressed in ciliary body from all donors, with apparent interindividual variability in protein levels. Consistent with our hypothesis, OAT1 and OAT3 appeared to localize to basolateral membranes of non-pigmented epithelial cells. Although we were unsuccessful in immunolocalizing NaDC3 to ciliary body, George et al., (George et al., 2004) showed by in situ hybridization that NaDC3 mRNA is contained within non-pigmented epithelial cells. Thus, we speculate that NaDC3 localizes to basolateral membranes of non-pigmented epithelium along with OAT1 and OAT3, similar to the kidney tubule. MRP4 localized to basolateral membranes of pigmented cells. The pattern of localization for the transporters examined is entirely consistent with the direction of active OA transport supported by the ciliary body, and its sensitivity to probenecid and novobiocin.

4.5 Predicted Elimination

From the data generated, and knowledge of anterior chamber physiology, we are able to model the rates of PAH elimination from the living eye, and the effects of active

transport, probenecid inhibition and passive outflow following the hypothetical administration of 1 mM PAH to aqueous humor. As mentioned earlier, the ciliary body produces and secretes aqueous humor into the anterior chamber of the eye (aqueous humor inflow). To maintain normal intraocular pressure and the optical properties of the globe, a balance between aqueous humor inflow by the ciliary body and passive outflow via the trabecular meshwork is required. In other words, the rate of aqueous humor inflow is equal to the rate of aqueous humor outflow in the normal healthy eye. The rate of aqueous humor inflow ranges from 1.5 – 3.0 $\mu l\ min^{-1}$ according to a circadian rhythm that is thought to be regulated by endogenous catecholamines, such as epinephrine and norepinephrine (Eakins and Ryan, 1964;Caprioli and Sears, 1984;Cooper et al., 1984;Farahbakhsh, 2003;Zhong et al., 2013). Using the net active steady-state PAH flux value (50 $nmoles \cdot cm^{-2} \cdot h^{-1}$) obtained from our Ussing chamber experiments (**Figure 3.3**), the surface area of the human ciliary body (6 cm^2, (Caprioli J, 1992)), and the volume of aqueous humor in human eye (0.25 ml, (Caprioli J, 1992)), the rate of PAH elimination passively via the outflow pathway and actively by the ciliary body can be estimated using equation 1 and equation 2, respectively (**Figure 4.1**). Based on the rate of passive aqueous humor outflow, using a value of 2 $\mu l\ min^{-1}$ (i.e., 120 $\mu l \cdot h^{-1}$) the rate of passive elimination of 1 mM PAH via the trabecular meshwork is 0.12 $\mu moles \cdot h^{-1}$. The rate of active PAH elimination out of the aqueous humor across the ciliary body is 0.3 $\mu moles \cdot h^{-1}$, a rate ~3-fold higher than passive outflow. Thus, the anticipated combined passive and active rate of PAH elimination from the aqueous humor is 0.42 $\mu moles \cdot h^{-1}$. Since there is 0.25 μmoles of PAH in the aqueous humor (equation 3, **Figure 4.1**), and it is eliminated at a rate of 0.42 $\mu moles \cdot h^{-1}$ (considering both active and

passive elimination), it would take 36 minutes to eliminate 1 mM PAH from the aqueous humor (considering elimination rate does not change with PAH concentration in aqueous humor, i.e., steady-state conditions) (equation 4, **Figure 4.1**). Also, the effect of probenecid on the amount of time it takes to eliminate PAH can be estimated from the functional studies shown in **Figure 3.4**. At steady-state the net active PAH flux in the presence of probenecid was 2 nmoles $\cdot$ cm^{-2} $\cdot$ h^{-1}. This equates to an elimination rate of 0.012 μmoles $\cdot$ h^{-1} (equation 5, **Figure 4.1**). In the presence of probenecid, the elimination rate of PAH should approximate 0.132 μmoles $\cdot$ h^{-1} (combined influence of active transport and passive outflow). Thus, in the presence of probenecid it would take 113 minutes to eliminate the PAH from the aqueous humor, ~3-fold longer than in its absence (equation 6, **Figure 4.1**). Interestingly, the half-life of iodopyracet (structurally similar to PAH) after intravitreal injection of rabbits increased ~3-fold by concomitant administration of probenecid (Forbes and Becker, 1960). In the monkey eye injected intravitreally with the antibiotics carbenecillin and cefazolin, administration of probenecid increased their vitreal half-lives 2-fold and ~4-fold, respectively (Barza et al., 1983).

4.6 Proposed Mechanism of Ocular Organic Anion Elimination

Based on the transport observed and the pattern of localization the following model of OA transport across the ciliary body, from aqueous humor-to-blood, is proposed (**Figure 4.2**). Similar to renal proximal tubule, OAT1, OAT3 and NaDC3 occur in basolateral membranes of non-pigmented epithelial cells and operate via a tertiary active

transport mechanism to mediate cellular OA uptake (Pelis and Wright, 2011). The first step in this process is generation of the Na-gradient by Na,K-ATPase, followed by the Na-dependent uptake of α-ketoglutarate (a Kreb's Cycle intermediate) by NaDC3. Although we were unsuccessful in immunolocalizing NaDC3 to ciliary body, George et al (George et al., 2004) showed by in situ hybridization that NaDC3 mRNA is contained within non-pigmented epithelial cells, where it could occur in either apical or basolateral membranes. Regardless of its localization, it is expected to establish an outwardly-directed α-ketoglutarate concentration gradient thus energizing OA uptake via an exchange mechanism on OAT1 and OAT3. Once inside non-pigmented epithelial cells OAs are pumped across the apical membrane into the intercellular space by MRP2, which localizes to this membrane (Pelis et al., 2009). Once in the intercellular space OAs can enter the choroidal blood supply by diffusing between the leaky junctions between pigmented cells. This is possible since large molecular weight tracers, such as horseradish peroxidase, when injected intravenously diffuse out of the choroidal blood supply and into the intercellular junction between adjacent pigmented cells and between the apical junction of pigmented and non-pigmented cells (Freddo, 2001). Alternatively, OAs can diffuse through gap junctions connecting non-pigmented and pigmented cells for final efflux into the interstitium by MRP4 located on basolateral membranes of pigmented cells. The currently accepted model for aqueous humor secretion by the ciliary body involves the movement of solutes between pigmented and non-pigmented cells through gap junctions (Do and Civan, 2004). Future work should be directed at confirming this model, for example, by using Na,K-ATPase, NaDC3 and MRP inhibitors

While the proposed model is limited to OAT1, OAT3, NaDC3, MRP2 and MRP4, there are likely other OA transporters functioning in aqueous humor-to-blood flux of OAs. Indeed, our microarray screen show that the human ciliary body expresses a variety of OA transporters, including OATP4A1, OATP3A1, OATP2A1, OATP2B1, MRP2, MRP3, MRP5 and P-gp, and probably OATP5A1, OATP1C1 and OATP1A2, although these signals were weak. Indeed, we previously showed that the human ciliary body expresses protein for P-gp, BCRP, MRP2 as well as MRP1 (Pelis et al., 2009), and others have shown protein expression for OATP1A2, OATP1C1, OATP2B1, OATP3A1 and OATP4A1 in human ciliary body (Gao et al., 2005). Given the tendency for overlap in ligand selectivity of OA transporters, we cannot rule out the possibility that in addition to OAT1, OAT3 and MRP4, that other OA transporters contributed to transepithelial OA flux across the ciliary body observed here. The microarray data also show that other ocular tissues express a variety of OA transporters, which likely contribute to OA disposition eye.

Rate of aqueous humor production in healthy human eye = 0.12 ml · h^{-1}

Volume of aqueous humor = 0.25 ml

Surface area of human ciliary body = 6 cm^2

Net active PAH flux at steady state = 50 nmoles · cm^{-2} · h^{-1}

Net active PAH flux at steady state with probenecid = 2 nmoles · cm^{-2} · h^{-1}

PAH concentration in aqueous humor compartment = 1 mM/L

Equation 1: Rate of PAH elimination via passive outflow

$$0.00012 \frac{L}{h} \times \ 1 \frac{mmoles}{L} = \mathbf{0.12\ \mu moles \cdot h^{-1}}$$

Equation 2: Rate of PAH elimination via active transport

$$50 \frac{nmoles}{cm^2 \times h} \times \ 6\ cm^2 = \mathbf{0.3\ \mu moles \cdot h^{-1}}$$

Equation 3: Amount of PAH in aqueous humor

$$0.001 \frac{moles}{L} \times \ 0.00025\ \text{L} = \mathbf{0.25\ \mu moles}$$

Equation 4: Amount of time to eliminate 0.25 µmoles PAH from aqueous humor

$$0.25\ \mu\text{moles} \div \ 0.42 \frac{\mu moles}{h} = \mathbf{36\ minutes}$$

Equation 5: Rate of PAH elimination via active transport in presence of probenecid

$$2 \frac{nmoles}{cm^2 \times h} \times \ 6\ cm^2 = \mathbf{0.012\ \mu moles \cdot h^{-1}}$$

Equation 6: Amount of time to eliminate 0.25 µmoles PAH from aqueous humor with probenecid

$$0.25\ \mu\text{moles} \div \ 0.132 \frac{\mu moles}{h} = \mathbf{113\ minutes}$$

Figure 4.1. The effects of active transport, probenecid inhibition and passive outflow. Rates of PAH elimination from the living eye following the hypothetical administration of 1 mM PAH to aqueous humor are calculated based on the data generated and knowledge of anterior chamber physiology

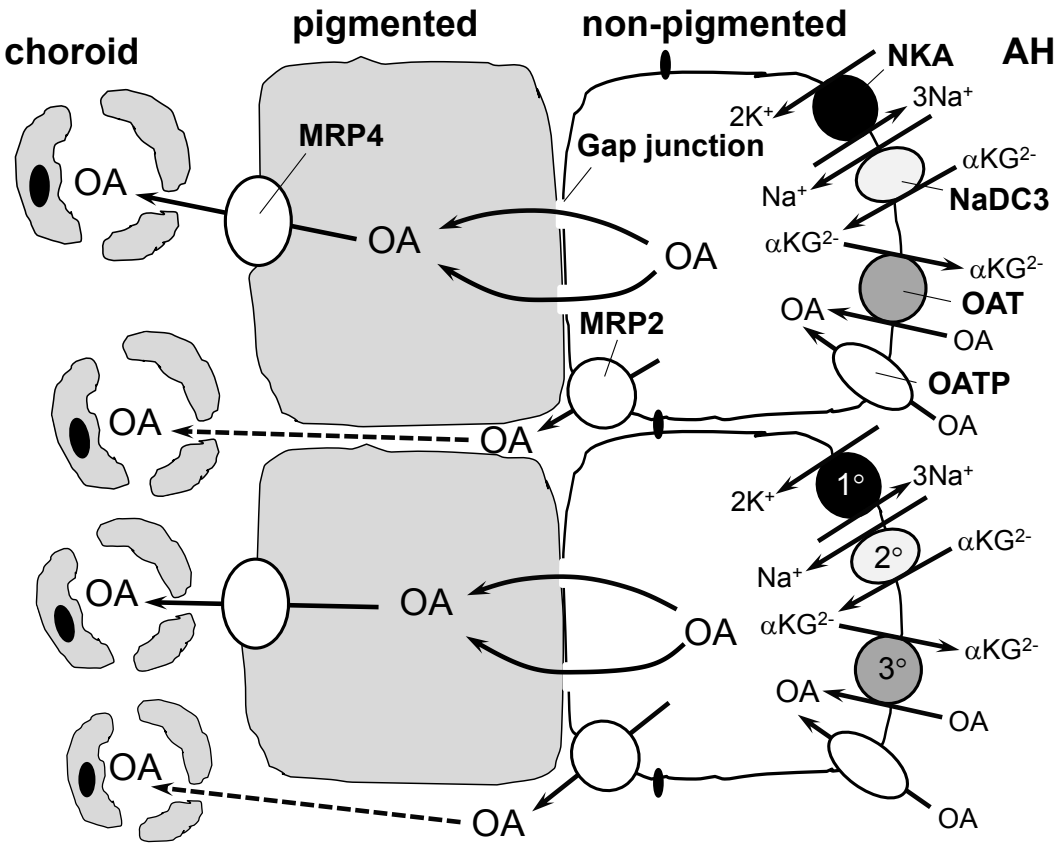

Figure 4.2. Hypothetical model of the involvement of NaDC3, OAT1, OAT3, MRP2 and MRP4 in transepithelial OA transport across the ciliary body, aqueous humor (AH)-to-blood (choroid). Uptake of OA across the basolateral membrane of non-pigmented cells occurs via a tertiary active transport process involving Na,K-ATPase (1°; NKA), NaDC3 (2°) and OAT1 and/or OAT3 (3°). OA are then pumped into the interstitium by MRP2, which localizes to apical membranes of non-pigmented cells. Alternatively, OAs diffuse through gap junctions into pigmented cells and are pumped into the interstitium by MRP4. MRP2 and MRP4 are ATP-dependent efflux transporters. mRNA for NaDC3 has been detected in non-pigmented epithelial cells (George et al., 2004), but its subcellular localization is unknown. It is placed in the basolateral membrane of non-pigmented cells in this model given that it trafficks to basolateral membranes of other epithelial cells. Other OA transporters may also contribute to transepithelial OA secretion. OATPs are included in the model since several OATPs have been localized to the basolateral membrane of non-pigmented epithelium (Gao et al., 2005). The subcellular distribution of other OA transporters in ciliary epithelium is unknown, so they are not included in this model.

CHAPTER 5: CONCLUSION

Ocular diseases range from mild to severe and can significantly impact quality of life. For many of these diseases there are small molecule therapeutic drugs that are effective for treatment, but delivering them to their target site inside of the eye is often challenging. The blood ocular barriers include the cornea, blood-aqueous humor barrier and blood-retinal barrier. There is increasing evidence that drug transporters present in tissues comprising these barriers contribute to drug disposition in the eye, with the potential to either reduce or increase ocular drug bioavailablity. A better understanding of the cellular and subcellular expression of drug transporters in ocular tissues, and their function in the tissue distribution of drugs in the eye, moves toward more effective strategies to deliver drugs to intraocular tissues.

Many drugs used to treat eye diseases are OAs at physiological pH, such as antibiotics, antivirals, nonsteroidal anti-inflammatory drugs, prostaglandin analogs and chemotherapeutics. Systemically, many of these OAs are eliminated from plasma by renal proximal tubular secretion involving the concerted activity of OA transporters in proximal tubule cells. Although there are in vivo and in vitro data suggesting that the ciliary body contributes to OA elimination from the eye, the molecular mechanisms have not been elucidated.

Here we showed that OAT1, OAT3, NaDC3 and MRP4 are expressed in the ciliary body epithelium of the human and we determined their subcellular localization. OAT1, OAT3 and NaDC3 are at the basolateral membrane of non-pigmented epithelial cells and in the position to facilitate organic anion uptake from aqueous humor to cell.

MRP4 is present in the membrane facing the choroidal blood supply, and given that it is an efflux transporter it likely pumps organic anions into the blood. The net active transport of *para*-aminohippurate and estrone-3-sulfate, and the effects of OAT/MRP inhibitors is consistent with the contention that the concerted activity of these transporters contribute to organic anion elimination from the aqueous humor. The pharmacokinetic implication of this process is that it would likely reduce drug half-life in the eye, either necessitating higher dosing or the need for more frequent dosing. Perhaps adjuvants, such as probenecid, which are relatively safe when given systemically, could be used to increase organic anion half-life in the aqueous humor. While active organic anion transport by the ciliary body has clear pharmacological implications, it is not yet clear what, if any, physiological significance this process may have. The lens is avascular and dependent on aqueous humor for both delivery of nutrients as well as removal of metabolic waste products. Perhaps, organic anion transport by the ciliary body contributes to removal of metabolic wastes that are organic anions.

The microarray data lends clues to other transporters that are expressed in the ciliary body. Interestingly, organic cation transporters important for the hepatic and renal elimination of drugs are present, leading to speculation that like organic anion transporters, they contribute to organic cation elimination from the eye. This would have implications for the ocular disposition of select drugs used to treat glaucoma, including β-adrenergic agonists and carbonic anhydrase inhibitors. Other transporters of immediate interest are the peptide transporters (PEPTs). Aqueous humor contains protein that is involved in absorbing ultraviolet radiation, which may protect against cataract. However,

it is not clear how the protein gets into aqueous humor or how it is cleared. Perhaps PEPTs in the ciliary body help regulate peptide levels in aqueous humor.

REFERENCES

Ahmed I, Gokhale R D, Shah M V and Patton T F (1987) Physicochemical Determinants of Drug Diffusion Across the Conjunctiva, Sclera, and Cornea. *J Pharm Sci* **76**:583-586.

Ahmed I and Patton T F (1985) Importance of the Noncorneal Absorption Route in Topical Ophthalmic Drug Delivery. *Invest Ophthalmol Vis Sci* **26**:584-587.

Al-Ghananeem AM and Crooks P A (2007) Phase I and Phase II Ocular Metabolic Activities and the Role of Metabolism in Ophthalmic Prodrug and Codrug Design and Delivery. *Molecules* **12**:373-388.

Alm A (1992) Ocular Circulation, in *Adler's Physiology of the Eye* (Hart WJ ed) pp 198-227, Mosby-Year Book, Inc, St. Louis.

Anand BS and Mitra A K (2002) Mechanism of Corneal Permeation of L-Valyl Ester of Acyclovir: Targeting the Oligopeptide Transporter on the Rabbit Cornea. *Pharm Res* **19**:1194-1202.

Anzenbacher P and Anzenbacherova E (2001) Cytochromes P450 and Metabolism of Xenobiotics. *Cell Mol Life Sci* **58**:737-747.

Asakura T and Shichi H (1992) Cytochrome P450-Mediated Prostaglandin Omega/Omega-1 Hydroxylase Activities in Porcine Ciliary Body Epithelial Cells. *Exp Eye Res* **55**:377-384.

Bainbridge JW, Raina J, Shah S M, Ainsworth J and Pinching A J (1999) Ocular Complications of Intravenous Cidofovir for Cytomegalovirus Retinitis in Patients With AIDS. *Eye (Lond)* **13**:353-356.

Barany EH (1976) Organic Cation Uptake in Vitro by the Rabbit Iris-Ciliary Body, Renal Cortex, and Choroid Plexus. *Invest Ophthalmol* **15**:341-348.

Barar J, Javadzadeh A R and Omidi Y (2008) Ocular Novel Drug Delivery: Impacts of Membranes and Barriers. *Expert Opin Drug Deliv* **5**:567-581.

Barza M, Kane A and Baum J (1982) The Effects of Infection and Probenecid on the Transport of Carbenicillin From the Rabbit Vitreous Humor. *Invest Ophthalmol Vis Sci* **22**:720-726.

Barza M, Kane A and Baum J (1983) Pharmacokinetics of Intravitreal Carbenicillin, Cefazolin, and Gentamicin in Rhesus Monkeys. *Invest Ophthalmol Vis Sci* **24**:1602-1606.

Becker B (1960) The Transport of Organic Anions by the Rabbit Eye. I. In Vitro Iodopyracet (Diodrast) Accumulation by Ciliary Body-Iris Preparations. *Am J Ophthalmol* **50:862-7.**:862-867.

Becker B and Forbes M (1961) Iodopyracet (Diodrast) Transport by the Rabbit Eye. *Am J Physiol* **200**:461-464.

Becker U, Ehrhardt C, Daum N, Baldes C, Schaefer U F, Ruprecht K W, Kim K J and Lehr C M (2007) Expression of ABC-Transporters in Human Corneal Tissue and the Transformed Cell Line, HCE-T. *J Ocul Pharmacol Ther* **23**:172-181.

BenEzra D and Maftzir G (1990) Ocular Penetration of Cyclosporin A. The Rabbit Eye. *Invest Ophthalmol Vis Sci* **31**:1362-1366.

Bito LZ (1972) Accumulation and Apparent Active Transport of Prostaglandins by Some Rabbit Tissues in Vitro. *J Physiol* **221**:371-387.

Campbell M and Humphries P (2012) The Blood-Retina Barrier: Tight Junctions and Barrier Modulation. *Adv Exp Med Biol* **763**:70-84.

Caprioli J (1992) The Ciliary Epithelia and Aqueous Humor, in *Adler's Physiology of the Eye* (Hart WM Jr ed) pp 228-247, Mosby YearBook, St. Louis.

Caprioli J and Sears M (1984) The Adenylate Cyclase Receptor Complex and Aqueous Humor Formation. *Yale J Biol Med* **57**:283-300.

Chavarria-Soley G, Sticht H, Aklillu E, Ingelman-Sundberg M, Pasutto F, Reis A and Rautenstrauss B (2008) Mutations in CYP1B1 Cause Primary Congenital Glaucoma by Reduction of Either Activity or Abundance of the Enzyme. *Hum Mutat* **29**:1147-1153.

Chen C, Stock J L, Liu X, Shi J, Van Deusen J W, DiMattia D A, Dullea R G and de Morais S M (2008) Utility of a Novel Oatp1b2 Knockout Mouse Model for Evaluating the Role of Oatp1b2 in the Hepatic Uptake of Model Compounds. *Drug Metab Dispos* **36**:1840-1845.

Chen P, Chen H, Zang X, Chen M, Jiang H, Han S and Wu X (2013) Expression of Efflux Transporters in Human Ocular Tissues. *Drug Metab Dispos* **41**:1934-1948.

Choudhary D, Jansson I, Sarfarazi M and Schenkman J B (2008) Characterization of the Biochemical and Structural Phenotypes of Four CYP1B1 Mutations Observed in Individuals With Primary Congenital Glaucoma. *Pharmacogenet Genomics* **18**:665-676.

Cihlar T, Lin D C, Pritchard J B, Fuller M D, Mendel D B and Sweet D H (1999) The Antiviral Nucleotide Analogs Cidofovir and Adefovir Are Novel Substrates for Human and Rat Renal Organic Anion Transporter 1. *Mol Pharmacol* **56**:570-580.

Cohen AI (1992) The Retina, in *Adler's Physiology of the Eye* (Hart WJ ed) pp 579-615, Mosby-Year Book, St. Louis.

Constable PA, Lawrenson J G, Dolman D E, Arden G B and Abbott N J (2006) P-Glycoprotein Expression in Human Retinal Pigment Epithelium Cell Lines. *Exp Eye Res* **83**:24-30.

Cooper RL, Constable I J and Davidson L (1984) Catecholamines in Aqueous Humour of Glaucoma Patients. *Aust J Ophthalmol* **12**:345-349.

Coupland SE, Penfold P L and Billson F A (1994) Hydrolases of Anterior Segment Tissues in the Normal Human, Pig and Rat Eye: a Comparative Study. *Graefes Arch Clin Exp Ophthalmol* **232**:182-191.

Cundy KC (1999) Clinical Pharmacokinetics of the Antiviral Nucleotide Analogues Cidofovir and Adefovir. *Clin Pharmacokinet* **36**:127-143.

Cundy KC, Petty B G, Flaherty J, Fisher P E, Polis M A, Wachsman M, Lietman P S, Lalezari J P, Hitchcock M J and Jaffe H S (1995) Clinical Pharmacokinetics of Cidofovir in Human Immunodeficiency Virus-Infected Patients. *Antimicrob Agents Chemother* **39**:1247-1252.

Dahlin A, Geier E, Stocker S L, Cropp C D, Grigorenko E, Bloomer M, Siegenthaler J, Xu L, Basile A S, Tang-Liu D D and Giacomini K M (2013) Gene Expression Profiling of Transporters in the Solute Carrier and ATP-Binding Cassette Superfamilies in Human Eye Substructures. *Mol Pharm* **10**:650-663.

Dey S, Patel J, Anand B S, Jain-Vakkalagadda B, Kaliki P, Pal D, Ganapathy V and Mitra A K (2003) Molecular Evidence and Functional Expression of P-Glycoprotein (MDR1) in Human and Rabbit Cornea and Corneal Epithelial Cell Lines. *Invest Ophthalmol Vis Sci* **44**:2909-2918.

Dias C, Nashed Y, Atluri H and Mitra A (2002) Ocular Penetration of Acyclovir and Its Peptide Prodrugs Valacyclovir and Val-Valacyclovir Following Systemic Administration in Rabbits: An Evaluation Using Ocular Microdialysis and LC-MS. *Curr Eye Res* **25**:243-252.

Do CW and Civan M M (2004) Basis of Chloride Transport in Ciliary Epithelium. *J Membr Biol* **200**:1-13.

Doane MG, Jensen A D and Dohlman C H (1978) Penetration Routes of Topically Applied Eye Medications. *Am J Ophthalmol* **85**:383-386.

Doshi M, Marcus C, Bejjani B A and Edward D P (2006) Immunolocalization of CYP1B1 in Normal, Human, Fetal and Adult Eyes. *Exp Eye Res* **82**:24-32.

Duan P and You G (2009) Novobiocin Is a Potent Inhibitor for Human Organic Anion Transporters. *Drug Metab Dispos* **37**:1203-1210.

Eakins KE and Ryan S J (1964) THE ACTION OF SYMPATHOMIMETIC AMINES ON THE OUTFLOW OF AQUEOUS HUMOUR FROM THE EYE. *Br J Pharmacol Chemother* **23**:374-382.

Edward A and Prausnitz M R (2001) Predicted Permeability of the Cornea to Topical Drugs. *Pharm Res* **18**:1497-1508.

Eraly SA, Monte J C and Nigam S K (2004) Novel Slc22 Transporter Homologs in Fly, Worm, and Human Clarify the Phylogeny of Organic Anion and Cation Transporters. *Physiol Genomics*.

Erickson KK, Sundstrom J M and Antonetti D A (2007) Vascular Permeability in Ocular Disease and the Role of Tight Junctions. *Angiogenesis* **10**:103-117.

Farahbakhsh NA (2003) Purinergic Signaling in the Rabbit Ciliary Body Epithelium. *J Exp Zool A Comp Exp Biol* **300**:14-24.

Fischbarg J and Lim J J (1974) Role of Cations, Anions and Carbonic Anhydrase in Fluid Transport Across Rabbit Corneal Endothelium. *J Physiol* **241**:647-675.

Flugel C and Lutjen-Drecoll E (1988) Presence and Distribution of Na+/K+-ATPase in the Ciliary Epithelium of the Rabbit. *Histochemistry* **88**:613-621.

Forbes M and Becker B (1960) The Transport of Organic Anions by the Rabbit Eye. II. In Vivo Transport of Iodopyracet (Diodrast). *Am J Ophthalmol* **50:867-75.**:867-875.

Forbes M and Becker B (1961) The Transport of Organic Anions by the Rabbit Ciliary Body. IV. Acetazolamide and Rate of Aqueous Flow. *Am J Ophthalmol* **51:1047-51.**:1047-1051.

Freddo TF (2001) Shifting the Paradigm of the Blood-Aqueous Barrier. *Exp Eye Res* **73**:581-592.

Freddo TF, Bartels S P, Barsotti M F and Kamm R D (1990) The Source of Proteins in the Aqueous Humor of the Normal Rabbit. *Invest Ophthalmol Vis Sci* **31**:125-137.

Fujii S, Hayashi H, Itoh K, Yamada S, Deguchi Y and Kawazu K (2013) Characterization of the Carrier-Mediated Transport of Ketoprofen, a Nonsteroidal Anti-Inflammatory Drug, in Rabbit Corneal Epithelium Cells. *J Pharm Pharmacol* **65**:171-180.

Gao B, Huber R D, Wenzel A, Vavricka S R, Ismair M G, Reme C and Meier P J (2005) Localization of Organic Anion Transporting Polypeptides in the Rat and Human Ciliary Body Epithelium. *Exp Eye Res* **80**:61-72.

Gardiner SJ and Begg E J (2006) Pharmacogenetics, Drug-Metabolizing Enzymes, and Clinical Practice. *Pharmacol Rev* **58**:521-590.

Gaudana R, Ananthula H K, Parenky A and Mitra A K (2010) Ocular Drug Delivery. *AAPS J* **12**:348-360.

George RL, Huang W, Naggar H A, Smith S B and Ganapathy V (2004) Transport of N-Acetylaspartate Via Murine Sodium/Dicarboxylate Cotransporter NaDC3 and Expression of This Transporter and Aspartoacylase II in Ocular Tissues in Mouse. *Biochim Biophys Acta* **1690**:63-69.

Geroski DH and Edelhauser H F (2000) Drug Delivery for Posterior Segment Eye Disease. *Invest Ophthalmol Vis Sci* **41**:961-964.

Grass GM and Robinson J R (1988) Mechanisms of Corneal Drug Penetration. I: In Vivo and in Vitro Kinetics. *J Pharm Sci* **77**:3-14.

Ho ES, Lin D C, Mendel D B and Cihlar T (2000) Cytotoxicity of Antiviral Nucleotides Adefovir and Cidofovir Is Induced by the Expression of Human Renal Organic Anion Transporter 1. *J Am Soc Nephrol* **11**:383-393.

Hodson S and Miller F (1976) The Bicarbonate Ion Pump in the Endothelium Which Regulates the Hydration of Rabbit Cornea. *J Physiol* **263**:563-577.

Hosoya K, Makihara A, Tsujikawa Y, Yoneyama D, Mori S, Terasaki T, Akanuma S, Tomi M and Tachikawa M (2009) Roles of Inner Blood-Retinal Barrier Organic Anion Transporter 3 in the Vitreous/Retina-to-Blood Efflux Transport of P-Aminohippuric Acid, Benzylpenicillin, and 6-Mercaptopurine. *J Pharmacol Exp Ther* **329**:87-93.

Huang AJ, Tseng S C and Kenyon K R (1989) Paracellular Permeability of Corneal and Conjunctival Epithelia. *Invest Ophthalmol Vis Sci* **30**:684-689.

Imaoka T, Kusuhara H, Adachi M, Schuetz J D, Takeuchi K and Sugiyama Y (2007) Functional Involvement of Multidrug Resistance-Associated Protein 4 (MRP4/ABCC4) in the Renal Elimination of the Antiviral Drugs Adefovir and Tenofovir. *Mol Pharmacol* **71**:619-627.

Ingraham L, Li M, Renfro J L, Parker S, Vapurcuyan A, Hanna I and Pelis R M (2014) A Plasma Concentration of Alpha-Ketoglutarate Influences the Kinetic Interaction of Ligands With Organic Anion Transporter 1. *Mol Pharmacol* **86**:86-95.

Irish JM, III and Dantzler W H (1976) PAH Transport and Fluid Absorption by Isolated Perfused Frog Proximal Renal Tubules. *Am J Physiol* **230**:1509-1516.

Jancova P, Anzenbacher P and Anzenbacherova E (2010) Phase II Drug Metabolizing Enzymes. *Biomed Pap Med Fac Univ Palacky Olomouc Czech Repub* **154**:103-116.

Juntunen J, Jarvinen T and Niemi R (2005) In-Vitro Corneal Permeation of Cannabinoids and Their Water-Soluble Phosphate Ester Prodrugs. *J Pharm Pharmacol* **57**:1153-1157.

Kadam RS, Vooturi S K and Kompella U B (2013) Immunohistochemical and Functional Characterization of Peptide, Organic Cation, Neutral and Basic Amino Acid, and Monocarboxylate Drug Transporters in Human Ocular Tissues. *Drug Metab Dispos* **41**:466-474.

Karla PK, Quinn T L, Herndon B L, Thomas P, Pal D and Mitra A (2009) Expression of Multidrug Resistance Associated Protein 5 (MRP5) on Cornea and Its Role in Drug Efflux. *J Ocul Pharmacol Ther* **25**:121-132.

Kaye GI (1969) Stereologic Measurement of Cell Volume Fraction of Rabbit Corneal Stroma. *Arch Ophthalmol* **82**:792-794.

Kennedy BG and Mangini N J (2002) P-Glycoprotein Expression in Human Retinal Pigment Epithelium. *Mol Vis* **8**:422-430.

Kitano S and Nagataki S (1986) Transport of Fluorescein Monoglucuronide Out of the Vitreous. *Invest Ophthalmol Vis Sci* **27**:998-1001.

Klaassen CD and Aleksunes L M (2010) Xenobiotic, Bile Acid, and Cholesterol Transporters: Function and Regulation. *Pharmacol Rev* **62**:1-96.

Kondo M and Araie M (1994) Movement of Carboxyfluorescein Across the Isolated Rabbit Iris-Ciliary Body. *Curr Eye Res* **13**:251-255.

Koyano S, Araie M and Eguchi S (1993) Movement of Fluorescein and Its Glucuronide Across Retinal Pigment Epithelium-Choroid. *Invest Ophthalmol Vis Sci* **34**:531-538.

Krishna DR and Klotz U (1994) Extrahepatic Metabolism of Drugs in Humans. *Clin Pharmacokinet* **26**:144-160.

Kuno N and Fujii S (2011) Dry Age-Related Macular Degeneration: Recent Progress of Therapeutic Approaches. *Curr Mol Pharmacol* **4**:196-232.

Li J and Bluth M H (2011) Pharmacogenomics of Drug Metabolizing Enzymes and Transporters: Implications for Cancer Therapy. *Pharmgenomics Pers Med* **4**:11-33.

Litterst CL, Mimnaugh E G, Reagan R L and Gram T E (1975) Drug Metabolism by Microsomes From Extrahepatic Organs of Rat and Rabbit Prepared by Calcium Aggregation. *Life Sci* **17**:813-818.

Lojda Z, Cejkova J, Bolkova A and Havrankova E (1976) Uneven Distribution of Alkaline Phosphatase in Individual Layers of Rabbit and Ox Cornea. Histochemical and Biochemical Study. *Histochemistry* **49**:237-243.

Lungkaphin A, Lewchalermwongse B and Chatsudthipong V (2006) Relative Contribution of OAT1 and OAT3 Transport Activities in Isolated Perfused Rabbit Renal Proximal Tubules. *Biochim Biophys Acta* **1758**:789-795.

Lynch T and Price A (2007) The Effect of Cytochrome P450 Metabolism on Drug Response, Interactions, and Adverse Effects. *Am Fam Physician* **76**:391-396.

Malhotra M and Majumdar D K (2001) Permeation Through Cornea. *Indian J Exp Biol* **39**:11-24.

Malik P, Kadam R S, Cheruvu N P and Kompella U B (2012) Hydrophilic Prodrug Approach for Reduced Pigment Binding and Enhanced Transscleral Retinal Delivery of Celecoxib. *Mol Pharm* **9**:605-614.

Mannermaa E, Vellonen K S, Ryhanen T, Kokkonen K, Ranta V P, Kaarniranta K and Urtti A (2009) Efflux Protein Expression in Human Retinal Pigment Epithelium Cell Lines. *Pharm Res* **26**:1785-1791.

Mannermaa E, Vellonen K S and Urtti A (2006) Drug Transport in Corneal Epithelium and Blood-Retina Barrier: Emerging Role of Transporters in Ocular Pharmacokinetics. *Adv Drug Deliv Rev* **58**:1136-1163.

Moitra K and Dean M (2011) Evolution of ABC Transporters by Gene Duplication and Their Role in Human Disease. *Biol Chem* **392**:29-37.

Nobeschi L, Freymuller E and Smith R L (2006) Intercellular Junctions in Rabbit Eye Ora Serrata. *Anat Histol Embryol* **35**:287-292.

Noske W, Fromm M, Levarlet B, Kreusel K M and Hirsch M (1994) Tight Junctions of the Human Corneal Endothelium: Morphological and Electrophysiological Features. *Ger J Ophthalmol* **3**:253-257.

Pelis RM, Shahidullah M, Ghosh S, Coca-Prados M, Wright S H and Delamere N A (2009) Localization of Multidrug Resistance-Associated Protein 2 in the Nonpigmented Ciliary Epithelium of the Eye. *J Pharmacol Exp Ther* **329**:479-485.

Pelis RM and Wright S H (2014) SLC22, SLC44, and SLC47 Transporters--Organic Anion and Cation Transporters: Molecular and Cellular Properties. *Curr Top Membr* **73**:233-261.

Pelis RM and Wright S H (2011) Renal Transport of Organic Anions and Cations, in *Comprehensive Physiology* pp 1795-1835, John Wiley & Sons, Inc..

Pereira dS, I and Bernkop-Schnurch A (2014) Pre-Systemic Metabolism of Orally Administered Drugs and Strategies to Overcome It. *J Control Release* **192**:301-309.

Pournaras CJ, Rungger-Brandle E, Riva C E, Hardarson S H and Stefansson E (2008) Regulation of Retinal Blood Flow in Health and Disease. *Prog Retin Eye Res* **27**:284-330.

Prausnitz MR and Noonan J S (1998) Permeability of Cornea, Sclera, and Conjunctiva: a Literature Analysis for Drug Delivery to the Eye. *J Pharm Sci* **87**:1479-1488.

Ross D, Cohen A I and McDougal D B, Jr. (1975) Choline Acetyltransferase and Acetylcholine Esterase Activities in Normal and Biologically Fractionated Mouse Retinas. *Invest Ophthalmol* **14**:756-761.

Sakanaka K, Kawazu K, Nishida K, Nakamura J, Nakashima M, Nakamura T, Oshita A, Ichikawa N and Sasaki H (2006) Transport of Timolol and Tilisolol in Rabbit Corneal Epithelium. *Biol Pharm Bull* **29**:2143-2147.

Saneto RP, Awasthi Y C and Srivastava S K (1982) Glutathione S-Transferases of the Bovine Retina. Evidence That Glutathione Peroxidase Activity Is the Result of Glutathione S-Transferase. *Biochem J* **205**:213-217.

Sastry BV, Vidaver P S, Janson V E and Franks J J (1994) S-Adenosyl-L-Methionine-Mediated Enzymatic Methylations in the Rat Retinal Membranes. *J Ocul Pharmacol* **10**:253-263.

Schwartzman ML, Masferrer J, Dunn M W, McGiff J C and Abraham N G (1987) Cytochrome P450, Drug Metabolizing Enzymes and Arachidonic Acid Metabolism in Bovine Ocular Tissues. *Curr Eye Res* **6**:623-630.

Shahidullah M and Delamere N A (2014) Connexins Form Functional Hemichannels in Porcine Ciliary Epithelium. *Exp Eye Res* **118**:20-29.

Shanthaveerappa TR and Bourne G H (1964) MONOAMINE OXIDASE DISTRIBUTION IN THE RABBIT EYE. *J Histochem Cytochem* **12**:281-287.

Shichi H and Nebert D W (1982) Genetic Differences in Drug Metabolism Associated With Ocular Toxicity. *Environ Health Perspect* **44**:107-117.

Shuprisha A, Lynch R M, Wright S H and Dantzler W H (1999) Real-Time Assessment of a-Ketoglutarate Effect on Organic Anion Secretion in Perfused Rabbit Proximal Tubules. *Am J Physiol* **277**:F513-F523.

Sparks DL, Thomas T N and Buckholtz N S (1981) Monamine Oxidase Activity in Bovine Retina: Subcellular Distribution and Drug Sensitivities. *Neurosci Lett* **21**:201-206.

Steuer H, Jaworski A, Elger B, Kaussmann M, Keldenich J, Schneider H, Stoll D and Schlosshauer B (2005) Functional Characterization and Comparison of the Outer Blood-Retina Barrier and the Blood-Brain Barrier. *Invest Ophthalmol Vis Sci* **46**:1047-1053.

Stone RA (1979) The Transport of Para-Aminohippuric Acid by the Ciliary Body and by the Iris of the Primate Eye. *Invest Ophthalmol Vis Sci* **18**:807-818.

Su CC, Liu Y F, Li S Y, Yang J J and Yen Y C (2012) Mutations in the CYP1B1 Gene May Contribute to Juvenile-Onset Open-Angle Glaucoma. *Eye (Lond)* **26**:1369-1377.

Sugiki S, Constant M A and Becker B (1961) In Vitro Accumulation of Chlorphenol Red by Rabbit Ciliary Body. *J Cell Comp Physiol* **58:181-3.**:181-183.

To CH, Mok K H, Do C W, Lee K L and Millodot M (1998) Chloride and Sodium Transport Across Bovine Ciliary Body/Epithelium (CBE). *Curr Eye Res* **17**:896-902.

Tornquist P, Alm A and Bill A (1990) Permeability of Ocular Vessels and Transport Across the Blood-Retinal-Barrier. *Eye (Lond)* **4**:303-309.

Tsuboi S and Pederson J E (1986) Permeability of the Isolated Dog Retinal Pigment Epithelium to Carboxyfluorescein. *Invest Ophthalmol Vis Sci* **27**:1767-1770.

Uwai Y, Ida H, Tsuji Y, Katsura T and Inui K (2007) Renal Transport of Adefovir, Cidofovir, and Tenofovir by SLC22A Family Members (HOAT1, HOAT3, and HOCT2). *Pharm Res* **24**:811-815.

van Aubel RA, Smeets P H, Peters J G, Bindels R J and Russel F G (2002) The MRP4/ABCC4 Gene Encodes a Novel Apical Organic Anion Transporter in Human Kidney Proximal Tubules: Putative Efflux Pump for Urinary CAMP and CGMP. *J Am Soc Nephrol* **13**:595-603.

Vasiliou V and Gonzalez F J (2008) Role of CYP1B1 in Glaucoma. *Annu Rev Pharmacol Toxicol* **48**:333-358.

Vellonen KS, Mannermaa E, Turner H, Hakli M, Wolosin J M, Tervo T, Honkakoski P and Urtti A (2010) Effluxing ABC Transporters in Human Corneal Epithelium. *J Pharm Sci* **99**:1087-1098.

Volotinen M, Maenpaa J, Kankuri E, Oksala O, Pelkonen O, Nakajima M, Yokoi T and Hakkola J (2009) Expression of Cytochrome P450 (CYP) Enzymes in Human Nonpigmented Ciliary Epithelial Cells: Induction of CYP1B1 Expression by TCDD. *Invest Ophthalmol Vis Sci* **50**:3099-3105.

Vooturi SK, Kadam R S and Kompella U B (2012) Transporter Targeted Gatifloxacin Prodrugs: Synthesis, Permeability, and Topical Ocular Delivery. *Mol Pharm* **9**:3136-3146.

Xiang CD, Batugo M, Gale D C, Zhang T, Ye J, Li C, Zhou S, Wu E Y and Zhang E Y (2009) Characterization of Human Corneal Epithelial Cell Model As a Surrogate for Corneal Permeability Assessment: Metabolism and Transport. *Drug Metab Dispos* **37**:992-998.

Yang B and Smith D E (2013) Significance of Peptide Transporter 1 in the Intestinal Permeability of Valacyclovir in Wild-Type and PepT1 Knockout Mice. *Drug Metab Dispos* **41**:608-614.

Yang H, Xun Y, Li Z, Hang T, Zhang X and Cui H (2009) Influence of Borneol on in Vitro Corneal Permeability and on in Vivo and in Vitro Corneal Toxicity. *J Int Med Res* **37**:791-802.

Yasukawa T, Ogura Y, Sakurai E, Tabata Y and Kimura H (2005) Intraocular Sustained Drug Delivery Using Implantable Polymeric Devices. *Adv Drug Deliv Rev* **57**:2033-2046.

Zanger UM and Schwab M (2013) Cytochrome P450 Enzymes in Drug Metabolism: Regulation of Gene Expression, Enzyme Activities, and Impact of Genetic Variation. *Pharmacol Ther* **138**:103-141.

Zderic V, Clark J I, Martin R W and Vaezy S (2004) Ultrasound-Enhanced Transcorneal Drug Delivery. *Cornea* **23**:804-811.

Zhang T, Xiang C D, Gale D, Carreiro S, Wu E Y and Zhang E Y (2008) Drug Transporter and Cytochrome P450 MRNA Expression in Human Ocular Barriers: Implications for Ocular Drug Disposition. *Drug Metab Dispos* **36**:1300-1307.

Zhang X, Groves C E, Bahn A, Barendt W M, Prado M D, Rödiger M, Chatsudthipong V, Burckhardt G and Wright S H (2004) Relative Contribution of OAT and OCT Transporters to Organic Electrolyte Transport in Rabbit Proximal Tubule. *Am J Physiol Renal Physiol*.

Zhao C and Shichi H (1995) Immunocytochemical Study of Cytochrome P450 (1A1/1A2) Induction in Murine Ocular Tissues. *Exp Eye Res* **60**:143-152.

Zhong Y, Yang Z, Huang W C and Luo X (2013) Adenosine, Adenosine Receptors and Glaucoma: an Updated Overview. *Biochim Biophys Acta* **1830**:2882-2890.